

18 Anyangcheon-Ro 1071, Yangchon-Gu,
 19 Seoul 07985, South Korea
 20 Tel: + 82 2 2650 5738 (Office), + 82 10 7222 5738 (Cell)
 21 Fax: + 82 2 2650 5591
 22 E-mail: jyseoh@ewha.ac.kr

23

24 Professor Byung-In Moon, MD, PhD
 25 Department of Surgery,
 26 Ewha Womans University Graduate School of Medicine,
 27 Anyangcheon-Ro 1071, Yangchon-Gu,
 28 Seoul 07985, South Korea
 29 Tel: + 82 2 2650 5102 (Office), + 82 10 8724 0687 (Cell)
 30 Fax: + 82 2 2650 5591
 31 E-mail: mbit@ewha.ac.kr

32

33

Abstract

Obesity is the disease accumulating excessive fat in the body. The prevalence of obesity and related metabolic disorders is increasing every year worldwide. Immunologically, obesity is a chronic low-grade inflammatory state with the increase of M1 macrophages and decrease of regulatory T cells (Tregs). IL-2/anti-IL-2 complex (IL-2C) and hyperbaric oxygen (HBO) are known to expand Tregs *in vivo* and suppress inflammation. Therefore, in this study, IL-2C and HBO were investigated for the preventive effect of obesity and related metabolic disorders. Male C57BL/6 mice were fed with a high-fat diet (HFD) for 16 weeks, and counterparts were fed with a low-fat diet (LFD). At the end of the experiment, the body weight gain and impaired glucose metabolism, elevated levels of insulin and total cholesterol induced by HFD were improved by the individual or combination treatment with IL-2C and HBO. Histological examination of the epididymal white adipose tissue showed adipocyte hypertrophy and many crown-like structures in the HFD control groups. In addition, the liver showed the progression of non-alcoholic fatty liver disease (NAFLD) in the HFD control groups, but it was significantly improved by the individual or combination treatment with IL-2C and HBO.

53 As for the underlying mechanism, inflammation induced by obesity
54 was decreased, and HIF-1 α expression by adipocyte hypertrophy was also
55 reduced by the individual or combination treatment with IL-2C and HBO. In
56 addition, adipose tissue browning was activated in brown and inguinal
57 adipose tissue, and the expression of UCP-1 involved in the
58 thermogenesis was increased by the individual or combination treatment
59 with IL-2C and HBO. Overall, these results suggested that IL-2C and HBO
60 might be a new promising immunotherapy for the treatment of obesity and
61 related metabolic disorders by regulation of inflammation and activation of
62 adipose tissue browning.

64

Introduction

65 Obesity comes from an imbalance between energy uptake and
66 consumption [1]. It is the state of excessive fat accumulated in the body
67 and causes many adverse effects on the health. WHO reported more than
68 1.9 billion adults were overweight, and out of these over 650 million were
69 obese in 2016 [2]. Nowadays, this issue becomes more serious as obesity
70 is becoming more prevalent in children and adolescents [3]. Obesity is
71 associated with diverse metabolic disorders, including type 2 diabetes [4]
72 and non-alcoholic fatty liver disease (NAFLD) [5], vascular diseases
73 including atherosclerosis [6] and cardiovascular diseases [7], and several
74 cancers [8]. Ultimately, the obesity shortens lifespan. For the treatment of
75 obesity, the most effective and safe method is changing the dietary regime
76 and lifestyle [9], but it is not easy. In serious cases, medical and even
77 surgical interventions are considered [10]. However, there are many side
78 effects and complications [11, 12], and thus, it is still necessary to develop
79 safer alternative methods for the treatment of obesity.

80 Adipose tissue is important for the maintenance of life [13]. In the
81 past, it was simply thought of as an organ storing energy as a fat to
82 prepare for the future starvation. Nowadays, it is considered as an

83 endocrine organ capable to mediate biological effects on the metabolism
84 and inflammation [14]. Adipose tissues release adipokines such as various
85 hormones and cytokines that control energy balance by regulating
86 appetitive signals and metabolic activity [15]. On the other hand, adipose
87 tissue undergoes dynamic changes in response to stimuli such as the
88 nutritional status and temperature change. These stimuli induce
89 remodeling of the adipose tissue as well as change the size and number
90 of adipocytes [16]. There are two types of adipose tissues, white adipose
91 tissue (WAT) and brown adipose tissue (BAT) [17, 18]. Both the WAT and
92 BAT are involved in energy balance, but they are distinct in the anatomical
93 locations, morphology, functions, and regulations. Especially, uncoupling
94 protein (UCP-1) is mainly expressed in the BAT and play an important role
95 in the metabolic and energy balance, such as cold- or diet-induced non-
96 shivering thermogenesis [19]. Recently, the brown-like adipocytes were
97 discovered in the WAT and it was called as 'beige or brite' adipocytes [20].
98 It implies the increase in metabolic activity, and therefore, browning of
99 WAT may be a new strategy of anti-obesity therapy [21]. As obesity
100 progresses, adipose tissues exhibit various changes. Lipid metabolites in
101 the adipose tissues are accumulated by incomplete β -oxidation and
102 increase of esterification [22, 23]. Adipocyte hypertrophy and the decrease

103 of blood flow induce hypoxic condition in the adipose tissues and
 104 activation of the hypoxia-inducible factor-1 alpha (HIF-1 α). In addition,
 105 infiltration of inflammatory cells including adipose tissue macrophages
 106 (ATMs) and formation of crown-like structures around dead adipocytes
 107 were observed [24], implying chronic low-grade inflammation [25]. ATMs
 108 exist in the visceral adipose tissue (VAT) and other metabolic tissues
 109 (liver, skeletal muscles) and secrete pro-inflammatory cytokines such as
 110 IL-1 β , IL-6 and TNF- α [26]. These circulating cytokines result in insulin
 111 resistance and play a critical role in the metabolic dysfunction. In addition,
 112 obesity induces the conversion of M2 (or alternatively activated)
 113 macrophages into M1 (or classically activated) macrophages. On the other
 114 hand, regulatory T cells (Tregs), that play a critical role in the maintenance
 115 of immune homeostasis *in vivo*, are decreased in obese adipose tissues.
 116 Thus, it could be hypothesized that it can be reverse the altered
 117 composition of inflammatory cells by increasing the Tregs as well as
 118 decreasing the M1 macrophages by the individual or combination
 119 treatment with IL-2/anti-IL-2 complex (IL-2C) and HBO. IL-2 is an
 120 important cytokine for the survival and function of Tregs and *in vivo*
 121 injection of IL-2 can induce expansion of Tregs [27]. Meanwhile, the half-
 122 life of IL-2 is very short and is rapidly removed from the circulation via

123 renal clearance [28]. Therefore, the IL-2 coupled with an anti-IL-2
 124 monoclonal antibody (JES6-1A12) is a very effective method for the
 125 selective expansion of CD4⁺Foxp3⁺ Tregs. It might be related with
 126 masking of motifs binding with IL-2R β on cytotoxic T cells and NK cells as
 127 well as prolongation of half-life. IL-2C has been shown to suppress several
 128 autoimmune or inflammatory diseases through expanding CD4⁺Foxp3⁺
 129 Tregs [29-31]. Hyperbaric oxygen (HBO) is another way to expand CD4⁺
 130 Foxp3⁺ Tregs [32, 33]. HBO is breathing of 100% oxygen with increased
 131 atmospheric pressure (2 - 3 ATA). During the treatment, the arterial
 132 oxygen tension reached to almost 2,000 mmHg, and in the tissue about
 133 200 to 400 mmHg [34]. It was initially used for the treatment of arterial gas
 134 embolism [35] and decompression sickness. Nowadays, HBO is applied to
 135 the diverse diseases, and it has improved diseases and symptoms.
 136 Breathing greater than 1 ATA of oxygen can increase of reactive oxygen
 137 species (ROS) level in the tissue [36]. Slight transient elevation of ROS
 138 increases the number and function of Tregs and suppresses inflammation.
 139 These effects have been reported that HBO attenuated autoimmune
 140 diseases such as atopic dermatitis [37] and psoriasis [38] by increasing
 141 the number and function of Tregs *in vivo*. In addition, it has been also
 142 reported that HBO treatment attenuated obesity in an animal model and

143 improved altered glucose metabolism in obese and type 2 diabetic people
144 [39-41].

145 Thus, both the IL-2C and HBO may expand Tregs and suppress chronic
146 low-grade inflammatory status in obesity, and synergy can be anticipated.
147 Therefore, in the present study, the individual or combination treatment of
148 IL-2C and HBO were investigated for the preventive effects on obesity and
149 related metabolic disorders induced by a high-fat diet.

150 **Materials and methods**

151 **Mice**

152 This study was approved by the Institutional Animal Care and Use
153 Committee of Ewha Womans University Graduate School of Medicine
154 (IACUC approval number: 14-0263). Mice (C57BL/6, male, 6 weeks old)
155 were purchased from Central Lab Animal Inc. (Seoul, Korea). Mice were
156 housed in a specific pathogen-free facility at Ewha Womans University.
157 For animal care, a room was controlled with a 12 hours light/dark cycle,
158 50% humidity and *ad libitum* access to food and water treated with γ -
159 irradiation.

160 **Animal experiment**

161 Seven-week-old C57BL/6J male mice were used in the experiment.
162 Mice were fed with a high-fat diet (HFD, 60 kcal% fat diets, 5.24 kcal/g,
163 D12492, Research Diets, New Brunswick, NJ, USA) or a low-fat diet (LFD,
164 10 kcal% fat diets, 3.85 kcal/g, D12450B, Research Diets) for 16 weeks.
165 The specific aim of this experiment is to investigate if IL-2C and/or
166 hyperbaric oxygen (HBO), that are known to expand Tregs *in vivo*,
167 attenuate HFD-induced obesity and related metabolic disorders.

168 Accordingly, the mice in the LFD and HFD groups were further divided into
169 5 sub-groups treated with IL-2C, HBO or both, and the control groups
170 treated with none or PBS (vehicle for IL-2C). Each sub-group was
171 composed of 8 - 16 mice. Body weights and food intakes were measured
172 every week during the experiment. The IL-2C mixture was prepared by
173 mixing mouse recombinant (r) IL-2 (eBioscience, San Diego, CA, USA)
174 and anti-mouse IL-2 IgG (JES6-1A12, eBioscience) at a ratio of 1 : 5 in
175 PBS and was incubated at 37°C for 30 minutes with agitation. Each time,
176 the mixture of 1 µg of rIL-2 and 5 µg of anti-mouse IL-2 in a volume of 150
177 µl was injected intraperitoneally (IP). Injection of IL-2C was started from
178 the 3rd week, daily in 3 consecutive days and then followed by once a
179 week until the end of the experiment. A hyperbaric oxygen chamber for
180 animal study was purchased from Particla (Daejeon, South Korea). The
181 HBO protocol was conducted with 100% O₂ at 3 ATA for 90 minutes after
182 20 minutes of compression, and then followed by 60 minutes of
183 decompression. HBO treatment was given 5 times a week from the start to
184 the end of the experiment. At the 14th week of the experiment,
185 intraperitoneal glucose tolerance test (IPGTT), and at the 15th week,
186 intraperitoneal insulin tolerance test (IPITT) were done. At the 16th week,
187 the mice were ethically sacrificed under general anesthesia, and spleen,

188 liver and adipose tissues were dissected for histological and
189 immunological study. For the study of WAT, epididymal white adipose
190 tissues (eWAT) were dissected. For the BAT, interscapular brown adipose
191 tissues (iBAT) were dissected. For the subcutaneous white adipose tissue,
192 anterior subcutaneous adipose tissues were dissected from the upper left
193 ventral region and inguinal subcutaneous adipose tissues were dissected.

194 **Glucose metabolism study**

195 For the glucose tolerance tests (GTT), mice were intraperitoneally
196 (IP) injected with 2 g/kg glucose (Sigma Aldrich, Saint Louis, MO, USA)
197 after fasting for 15 hours. Blood glucose levels were measured with a
198 glucometer (Accu-Check Performa kit, Roche, Basel, Switzerland) at 0, 15,
199 30, 60 and 120 minutes. For the insulin tolerance tests (ITT), mice were IP
200 administered with 0.75 IU/kg insulin glargine (Lantus™, Sanofi, Paris,
201 France) after fasting for 4 hours, and blood glucose levels were measured
202 at 0, 15, 30, 60 and 120 minutes. The area under the curve (AUC) was
203 calculated by PRISM program v5.01 (GraphPad Software Inc., La Jolla,
204 CA, USA). Insulin levels in fasting sera were measured by using an insulin
205 ELISA kit (ALPCO, Salem, NH, USA).

206 **Biochemical tests for lipid**

207 Serum levels of total cholesterol (TC) and triglyceride (TG) were
208 measured by using TC assay kit and serum TG quantification kit
209 purchased from Cell Biolabs, Inc. (San Diego, CA, USA) according to the
210 manufacturer's instructions.

211 **Histology**

212 **H&E, Masson's trichrome, Oil red O staining and** 213 **microscopic analysis**

214 The dissected tissue was fixed in 10% formalin. Serial sections (4
215 μm) were mounted on slides and stained with hematoxylin and eosin
216 (H&E). Adipocyte size and number of eWAT, as well as the thickness of
217 anterior subcutaneous WAT were measured by Image J program (National
218 Institutes of Health, Bethesda, MD, USA).

219 Masson's trichrome staining was applied for the detection of collagen
220 fibers in the liver tissues. Paraffin-embedded liver sections were stained
221 with Weigert's iron hematoxylin working solution (Polysciences inc.,
222 Warrington, PA, USA) for 10 minutes and then with Biebrich scarlet-acid
223 fuchsin solution (Sigma Aldrich) for 10 minutes. After washed with D.W.,
224 the sections were differentiated in phosphomolybdic-phosphotungstic acid

225 solution (Sigma Aldrich) for 10 minutes and were stained with aniline blue
226 solution (Sigma Aldrich) for 5 minutes. Then, the tissue samples were
227 dehydrated and mounted.

228 Oil red O staining was applied for the evaluation of fat accumulation
229 in the liver. Freshly dissected liver tissues were embedded in Tissue-Tek
230 O.C.T. compound (Thermo Fisher Scientific, MA, USA), and were frozen
231 at -196.5°C. The frozen sections (10 µm thickness) were prepared and
232 dried by air. The slides were rinsed with 60% isopropanol (Sigma Aldrich)
233 and were stained with Oil red O solution (Sigma Aldrich) for 15 minutes.
234 The slides were rinsed again with 60% isopropanol and were stained with
235 alum hematoxylin (Polysciences inc.). The slides were rinsed with D.W.
236 and were mounted with aqueous mount solution (Thermo Fisher
237 Scientific).

238 For the assessment of NAFLD activity score (NAS), randomly
239 selected 3 independent images were examined and scored for the
240 steatosis, lobular inflammation, and ballooning. The NAS is calculated by
241 the sum of scores for steatosis (0 - 3), lobular inflammation (0 - 3), and
242 hepatocyte ballooning (0 - 2), and the total score ranges from 0 to 8 [42].

244 **Immunohistochemistry and quantification of expression** 245 **levels**

246 The paraffin-embedded tissue sections (4 µm) were hydrated in
247 ethanol and D.W. Tissue slides were heated in boiling water to retrieve
248 antigens for 10 - 20 minutes. Endogenous peroxidase was blocked by
249 treatment with H₂O₂ containing peroxidase blocking reagent (DAKO, Santa
250 Clara, CA, USA) for 10 minutes in the dark. After washed, the sections
251 were treated with those primary antibodies such as F4/80 (Abcam,
252 Cambridge, UK, 1:100 dilutions), HIF-1α (Bethyl Laboratories, Inc.,
253 Montgomery, TX, USA, 1:100 dilutions), UCP-1 (Abcam, 1:4,000 dilutions)
254 for 1 - 2 hours at RT and then treated with HRP polymer (Cell Signaling
255 Technology, Inc., MA, USA) for 30 minutes. Then, the sections were
256 treated with DAB chromogen (Biocare Medical, Pacheco, CA, USA) for 5
257 minutes at RT in the dark and then stopped by D.W. The slides were
258 counter-stained with hematoxylin for 5 sec. Tissue sample was dehydrated
259 and mounted.

260 For the quantitative analysis of HIF-1α expression, the slides were
261 applied for high-resolution whole slide scan using the Vectra Polaris
262 (PerkinElmer Inc., Hopkinton, MA, USA). The regions for analysis were

263 randomly selected 3 - 5 spots and applied to the inForm (Image Analysis
264 Software, Perkin Elmer). Adipose and liver tissues were selected by tissue
265 and blank segmentation algorithm. Among those tissue areas, cell
266 segmentations were performed by nucleus intensity and cell morphology.
267 The inForm generated intensity reports for DAB markers from the each
268 analyzed cells. The DAB positive cells were measured in the selected 3 - 5
269 images per a group at the resolution of X10 in the eWAT and X20 in the
270 liver.

271 **Flow cytometry**

272 For the preparation of splenocytes, spleens were teased and
273 minced, and were treated with ACK solution (Sigma Aldrich) for 5 minutes
274 at RT, and then filtered through 70 µm cell strainers (SPL Life Sciences
275 Co., Korea). For enrichment, the cells were spun on a 17.5% Accudenz
276 (Accurate Chemical & Scientific, Westbury, NY, USA) density gradient
277 centrifugation (2,000 rpm, 20 minutes, 20°C). Interface layer and pellet
278 were used for the staining of macrophages and T cells, respectively.
279 Stromal vascular fractions (SVFs) were prepared from eWAT by using
280 adipose tissue dissociation kit (Miltenyi Biotec, Bergisch Gladbach,
281 Germany) according to the manufacturer's instruction. After the fractions

282 were prepared as single cells, they were stained for M1 macrophages and
 283 Tregs using anti-F4/80 FITC (BM8, eBioscience) and anti-CD11c PE (HL3,
 284 BD, Franklin Lakes, NJ, USA) after Fc blocking with anti-CD16/32
 285 antibodies (2.4G2, BD). The cells were also stained with anti-CD3
 286 PerCP/Cy5.5 (17A2, Biolegend, San Diego, CA, USA), anti-CD4 FITC
 287 (GK1.5, Biolegend) and anti-CD25 Brilliant Violet 711 (PC61, Biolegend)
 288 antibodies. For the staining of intranuclear FoxP3, the cells were
 289 permeabilized with FoxP3 staining buffer solution (eBioscience) and then
 290 stained with anti-FoxP3 APC (FJK-16s, eBioscience). The stained cells
 291 were analyzed using LSRFortessa (BD) and FlowJo software v10 (Tree
 292 Star, Ashland, OR, USA).

293 **Statistical analysis**

294 Results are presented as the mean \pm SEM. Statistical significance
 295 was evaluated with *t*-test and two-way ANOVA. Significance was set at *
 296 $p < 0.05$, ** $p < 0.01$, *** $p < 0.001$. The significance of each experimental
 297 group was evaluated by comparison with the control group.

Results

Attenuation of the body weight gain by the individual or combination treatment with IL-2C and HBO

Body weight gain was faster and more prominent in the HFD groups than in the LFD groups. Body weights in the HFD control group became heavier than in the LFD control group from the 4th week and the difference between the groups became progressively more prominent until the end of the experiment (S1 Fig). At the end of the experiment, the body weights in the groups treated with the individual or combination of the IL-2C and HBO were significantly lower than those in the controls of the HFD group (Fig 1A). In the LFD groups, at the end of the experiment, the body weights in the group by individual treatment with IL-2C and combination treatment were also significantly lower than those in the controls. The body weights in the group by individual treatment with HBO was also lower but was not statistically significant. There was no significant difference in the food intake between the experimental groups (Fig 1B).

Fig 1. Body weights and food intake. Body weights of the experimental groups at the end of the experiment (A). Food intake (B).

Improvement of impaired glucose metabolism and dyslipidemia by the individual or combination treatment with IL-2C and HBO

At the end of the experiment, blood glucose levels after fasting for 15 hours were significantly higher in the HFD control groups than in the LFD groups, suggesting hyperglycemia was induced (Fig 2A). Individual treatment with IL-2C or HBO decreased blood glucose levels, but without statistical significance, while combination treatment decreased it significantly. IPGTT showed delayed glucose clearance from the blood in the HFD control groups, suggesting dysregulation of glucose metabolism (Fig 2B). In the combination treatment groups, the blood glucose levels were significantly decreased starting from 30 minutes and from 60 minutes in each LFD and HFD compared to the control groups (Fig 2C and D). Glucose clearance rate after glucose injection was shortened by the individual or combination treatment with IL-2C and HBO (Fig 2E). In order to investigate if insulin functions appropriately, blood glucose levels were measured after IP injection of insulin. The blood glucose levels after fasting for 4 hours was significantly lower in the HFD groups by individual treatment with HBO or combination treatment (Fig 2F). The levels of blood glucose at 2 hours after insulin injection were showed significantly higher and delayed glucose clearance in the HFD control groups, therefore this result suggests the inappropriate function of insulin (Fig 2G). Individual or combination treatment with IL-2C and HBO decreased blood glucose levels after injection of insulin, especially combination treatment was significantly lower during 2 hours in the HFD groups, but there was no significant change in the LFD groups (Fig

2H and I). Therefore, glucose clearance rate after insulin injection was significantly improved by the individual or combination treatment with IL-2C and HBO in the HFD (Fig 2J). In addition, serum insulin levels after fasting for 15 hours were significantly higher in the HFD control groups (Fig 2K). *Albeit* at higher insulin levels, hyperglycemia was not corrected, suggesting insulin resistance was induced in the HFD control groups. Individual or combination treatment with IL-2C and HBO not only decreased fasting serum insulin levels in the HFD groups, in parallel with the decrease of fasting blood glucose levels but also enhanced glucose clearance from the blood after injection of insulin, suggesting improvement of insulin function. At the end of the experiment, hypercholesterolemia was induced in the HFD control groups, which was improved by the individual or combination treatment with IL-2C and HBO (Fig 2L). Meanwhile, serum triglyceride levels were not significantly different between the LFD and HFD groups (Fig 2M). Taken together, it was suggested that the individual or combination treatment with IL-2C and HBO improved impaired glucose metabolism and dyslipidemia induced by HFD.

Fig 2. Blood and biochemical tests to analysis of glucose and lipid metabolism.

IPGTT and IPITT were conducted in the experimental groups of LFD and HFD. Blood glucose levels at the start (after fasting for 15 hours) (A) and at the end (2 hours after glucose injection) (B) of IPGTT. The levels of blood glucose in the LFD (C) and HFD groups (D) during the 2 hours, and AUC of IPGTT (E). Blood glucose levels at the start (after fasting for 4 hours) (F) and at the end (2 hours after the insulin injection) (G) of IPITT. The levels of blood glucose in the LFD (H) and HFD

363 groups (I) during the 2 hours, and AUC of IPITT (J). The levels of insulin (K), total
 364 cholesterol (L) and triglyceride (M) in the sera after fasting for 15 hours.

Modulation of HFD-induced adipose tissue remodeling by the individual or combination treatment with IL-2C and HBO

As obesity progresses by HFD, adipose tissues undergo dynamic remodeling by changing the size and number of adipocytes. Histological examination of the eWAT showed many enlarged adipocytes in the HFD control groups, but many small or shrunken cells were also observed (Fig 3A). Around the small adipocytes, many inflammatory cells were infiltrated, showing many typical crown-like structures. The groups by the individual or combination treatment with IL-2C and HBO has scarcely observed the infiltration of inflammatory cells, and the size of adipocytes was rather homogenous with less variation in the eWAT. The size of adipocytes in the HFD control groups was larger than LFD groups (Fig 3B). It was decreased by the individual or combination treatment in both LFD and HFD groups. On the other hand, the size of the adipocytes in the HFD groups by individual treatment with IL-2C was not different from that in the control groups. Inversely proportional to size, the number of adipocytes in the HFD control groups decreased in the same area compared with the treatment groups (Fig 3C). For the evaluation of fat accumulation in the subcutaneous adipose tissue (SAT), anterior SAT thickness was measured from the ends of the dermis to muscle layer (Fig 3D and E). The depth of anterior SAT was also significantly thicker in the HFD control groups compared with the LFD groups. Meanwhile, it was significantly thinner in the LFD and HFD groups by combination treatment with IL-2C and HBO compared with that in the control groups. Therefore, HFD-induced adipose tissue remodeling was prevented in both VAT and

SAT by the individual or combination treatment with IL-2C and HBO.

Fig 3. Histological analysis of HFD-induced adipose tissue remodeling in the

VAT and SAT. H&E staining of eWAT (X200, scale bar is 100 μ m) shows

hypertrophic adipocytes and crown-like structures in the HFD control groups (A). The

groups by the individual or combination treatment with IL-2C and HBO has reduced

the size of adipocytes, and immune cells infiltration in the eWAT. Histological

analysis of the size (B) and number (C) of adipocytes was performed by ImageJ

program. H&E staining shows the side of longitudinally sectioned anterior SAT

(X100, scale bar is 200 μ m) (D). ‘Bidirectional arrows’ indicate adipose thickness

from the ends of the dermis to muscle layer. The thickness of anterior SAT was

analyzed using the ImageJ program by measuring the length of arrows mentioned

above (E).

Improvement of non-alcoholic fatty liver disease (NAFLD) by the individual or combination treatment with IL-2C and HBO

The liver plays important roles in the lipid metabolism such as import of serum FFAs and generation, store and then export of lipids and lipoproteins. In addition, it was reported that 80% of obese people have the NAFLD. Histological examination of the H&E stained liver sections in the HFD control groups showed severe steatosis with many microvesicular and macrovesicular fatty changes (Fig 4A). Oil red O staining showed more evident fat accumulation in the liver of the HFD control groups, but it was dramatically reduced by the individual or combination treatment with IL-2C and HBO (Fig 4B). According to the fat accumulation in the liver, the weight of liver was significantly increased by HFD, which were also significantly decreased by individual treatment with IL-2C and combination treatment, but not significantly with individual treatment with HBO (Fig 4C). There was no significant difference between in the LFD each group. In the HFD control groups, hepatocyte ballooning and Mallory-Denk bodies were also observed, suggesting degenerative changes of the liver (Fig 4D). Lobular inflammation by infiltration of polymorphonuclear leukocytes and lymphocytes also suggested ongoing hepatitis. Masson's trichrome staining shows slight but evident fibrotic changes (Fig 4E). Taken together, it could be argued that non-alcoholic steatohepatitis (NASH) has been induced by HFD, and semi-quantitative analysis also showed the significant increase of NAFLD activity score (NAS) in the HFD control groups (Fig 4F-I). Meanwhile, the histological characteristics of NASH were dramatically attenuated in

parallel with the significant decrease of NAS in the groups by the individual or combination treatment with IL-2C and HBO.

Fig 4. Histopathological analysis of NAFLD induced by HFD. H&E staining of the liver in the experimental groups (X200, scale bar is 100 μ m) (A). H&E staining shows severe steatohepatitis in the HFD control groups, but it was prevented in the groups by the individual or combination treatment with IL-2C and HBO. Oil red O staining (X200, scale bar is 100 μ m) (B) shows the fat depositions in the liver. Fat vacuoles stained red were overall scattered in the liver of HFD control groups, but the fat vacuoles by the individual or combination treatment with IL-2C and HBO become small and less. The weight of the liver (C). H&E staining of the HFD control groups (X400) (D). ‘Blue arrows’ indicate the Mallory-Denk bodies, ‘* and **’ indicate the microvesicular and macrovesicular fatty changes, and ‘Yellow arrow’ indicates lobular inflammation composed of PMLs and lymphocytes. Masson’s trichrome staining shows fibrotic changes in the HFD control groups (X400) (E). Semi-quantitative analysis was performed to assess of steatosis (F), lobular inflammation (G), and hepatocyte ballooning (H) for NAFLD activity score (NAS) (I).

Suppression of HFD-induced inflammation by the individual or combination treatment with IL-2C and HBO

IHC and flow cytometry was conducted to evaluate the inflammatory state induced by obesity. Firstly, the IHC study for the F4/80 was conducted with the analysis of the infiltrated macrophages in the eWAT. As a result, many macrophages composing the crown-like structures were infiltrated in the eWAT of the HFD control groups, but it was less in the mice treated with the individual or combination of IL-2C and HBO (Fig 5A and B). Flow cytometry was performed to evaluate the inflammatory state of adipose tissue and spleen, and the proportional changes of M1 macrophages and Tregs were examined locally and systemically. Flow cytometric analysis also showed the significant increase in F4/80⁺CD11c⁺ M1 macrophage proportion among the VSFs of eWAT in the HFD control groups (Fig 5C). Meanwhile, the proportion of M1 macrophage was significantly decreased by combination treatment with IL-2C and HBO. Individual treatment of IL-2C or HBO in the HFD groups were also decreased but without significance. Flow cytometric analysis of the splenocytes also showed the similar pattern of increase the M1 macrophage proportion in the HFD control groups and decrease by the individual or combination treatment with IL-2C and HBO, and the strength of statistical significance was stronger than eWAT (Fig 5D). In the eWAT as well as in the spleen, combination treatment with IL-2C and HBO in the HFD groups significantly reduced the proportion of M1 macrophage. The CD4⁺FoxP3⁺ Treg proportion in both eWAT and spleen of the HFD groups was significantly increased by the individual or combination treatment with IL-2C and HBO. The proportion of Treg among the VSFs of eWAT was significantly decreased in the HFD control groups compared with that in the LFD

groups (Fig 5E). In contrast, the proportion of Treg in the HFD groups was increased by the individual or combination treatment with IL-2C and HBO, and the proportion of Treg in the LFD groups increased only in the individual treatment with HBO. The proportion of Treg in the spleen of the HFD control groups was also decreased compared with the LFD groups (Fig 5F). It was significantly increased in both LFD and HFD groups by individual treatment with IL-2C and combination treatment. In summary, in both eWAT and spleen of the HFD control groups, M1 macrophages were increased whereas Tregs were decreased compared with the LFD control groups, suggesting the pro-inflammatory state. On the other hand, the individual or combination treatment with IL-2C and HBO reversely changed the proportion of the immune cells induced by HFD, suggesting suppression of the inflammatory responses.

Fig 5. Histopathology and immunological analysis of eWAT and spleen induced by HFD. IHC for F4/80 as a macrophages marker in the eWAT (X400, scale bar is 50 μ m) (A). Quantification of F4/80 positive macrophage cells count (B). Flow cytometry for M1 macrophages and Tregs population in the eWAT and spleen. F4/80 and CD11c double positive cells were gated as M1 macrophages in the eWAT (C), and spleen (D). CD4 and FoxP3 double positive cells in CD3⁺ T cells were gated as Tregs in the eWAT (E), and spleen (F).

Reduction of HIF-1 α expression in the eWAT and liver by the individual or combination treatment with IL-2C and HBO

Another cardinal manifestation of obesity is hypoxia in the WAT. IHC showed scarce expression of HIF-1 α in the eWAT of the LFD groups, which was significantly enhanced in the HFD control groups, suggesting hypoxic state (Fig 6A and B). The enhanced expression of HIF-1 α in the HFD control groups was significantly decreased to the comparable levels with that in the LFD groups by the individual or combination treatment with IL-2C and HBO, suggesting the normoxic state. IHC for HIF-1 α in the liver tissues showed a similar pattern of increase of HIF-1 α expression in the HFD control groups, which was decreased by the individual or combination treatment with IL-2C and HBO (Fig 6C and D).

Fig 6. Immunohistochemistry and analysis for HIF-1 α in the eWAT and liver.

Immunohistochemistry for HIF-1 α in the eWAT and quantification of HIF-1 α expression area. The left of the picture is the IHC staining image and the right paired picture is the analysis image (A). Quantification the ratio for HIF-1 α positive area compared with HFD control groups (B). Immunohistochemistry for HIF-1 α in the liver and quantification of HIF-1 α expression area. (C). Quantification the ratio for HIF-1 α positive area compared with HFD control groups (D).

Activation of adipose tissue browning by the individual or combination treatment with IL-2C and HBO

Histological examination of the iBAT showed small and multilocular features in the LFD groups (Fig 7A). In the HFD control groups, many unilocular hypertrophic adipocytes were observed with infiltration of inflammatory cells, suggesting whitening of adipose tissue. These histological features were less prominent by the individual or combination treatment with IL-2C and HBO of the HFD. The weight of iBAT was also slightly increased in the HFD control groups, compared with the LFD control groups, but without statistical significance (Fig 7B). In the mice treated with the combination of IL-2C and HBO, the weight of iBAT was significantly decreased in both LFD and HFD groups compared with each control groups. IHC showed that the uncoupling protein-1 (UCP-1) was intensely expressed in the iBAT of the LFD groups, which became more intense by the individual or combination treatment with IL-2C and HBO (Fig 7C and D). The UCP-1 expression in the iBAT of the HFD control groups was slightly less intense, which was also strengthened by the individual or combination treatment with IL-2C and HBO.

In addition, histological examination of the iWAT of the LFD groups showed homogeneous unilocular adipocytes, it was almost similar to those of eWAT (Fig 7E). However, many small multilocular adipocytes were observed by the individual or combination treatment with IL-2C and HBO. In the HFD control groups, iWAT showed many hypertrophic adipocytes along with the infiltration of inflammatory cells. The size of iWAT of the HFD by the individual or combination treatment with IL-2C and HBO were smaller than the HFD control groups. The weight of iWAT was

also decreased by combination treatment with IL-2C and HBO in the LFD groups (Fig 7F). In the HFD control groups, the weight of iWAT was remarkably increased compared with the LFD groups. It was restored to the comparable level with LFD by combination treatment with IL-2C and HBO. In addition, the expression of UCP-1 in the iWAT was scarcely expressed in the LFD control groups, but it was gradually increased by the individual or combination treatment with IL-2C and HBO (Fig 7G and H). It was higher by individual treatment with HBO in comparison to the individual treatment with IL-2C, and the combination treatment with IL-2C and HBO showed the highest increase in UCP-1 expression. UCP-1 expression was hardly observed in the HFD control groups, but it was only expressed in the group treated with combination of IL-2C and HBO. As a result, the whitening of the adipose tissue induced by the HFD was prevented by the individual or combination treatment with IL-2C and HBO, and it was activated the conversion to the browning of the adipose tissue.

Fig 7. H&E staining and Immunohistochemistry for observation of adipose tissue browning in the iBAT and iWAT. H&E staining of the iBAT (X200, scale bar is 100 µm) shows adipose tissue whitening by the histomorphologic change from the multilocular to unilocular and increase of immune cells infiltration in the HFD control groups (A). Inversely, the individual or combination treatment with IL-2C and HBO are less fat accumulation and immune cells infiltration in the iBAT. The weight of the iBAT (B). IHC for UCP-1 in the iBAT (X400, scale bar is 50 µm) (C). Quantification the ratio for UCP-1 positive area compared with HFD control groups (D). H&E staining of the iWAT (X200, scale bar is 100 µm) shows hypertrophic adipocytes and

550 immune cells infiltration in the HFD control groups, but it was reduced in the groups
 551 by the individual or combination treatment with IL-2C and HBO (E). In the LFD
 552 groups, adipose tissue browning was induced by individual treatment with IL-2C or
 553 HBO, and the group by combination treatment with IL-2C and HBO strongly induced
 554 browning. The weight of the iWAT (F). IHC for UCP-1 in the iWAT (X400, scale bar is
 555 50 μ m) (G). 'Arrows' indicate the UCP-1 expression. Quantification the ratio for UCP-
 556 1 positive area compared with HFD control groups (H).

Discussion

In the present study, the individual or combination treatment with IL-2C and HBO attenuated HFD-induced obesity and related metabolic disorders. The significant decrease of body weight gain by combination treatment with IL-2C and HBO was observed from as early as the 4th week in the HFD group, and from the 8th week in the LFD group. At the end of the experiment, decrease of body weight gain was as much as 21.2% and 20.1% in the HFD and LFD groups, respectively. Individual treatment with IL-2C or HBO also reduced weight gain, but the significant difference was always represented by combination treatment with IL-2C and HBO (S1 Table).

Impaired glucose metabolism in the HFD control groups was also improved by combination treatment with IL-2C and HBO. In the IPGTT, combination treatment with IL-2C and HBO not only significantly reduced the blood glucose levels both fasting, and 2 hours after glucose injection but also showed significantly decreased the AUC. In IPITT, blood glucose levels at 2 hours after insulin injection, AUC and fasting serum insulin levels were significantly decreased by individual treatment with IL-2C or HBO as well as by combination treatment. However, blood glucose levels after fasting for 4 hours were significantly decreased by individual treatment with HBO or combination treatment, but not by individual treatment with IL-2C. All the data presented in this study including body weight, blood glucose, serum insulin levels, and AUCs of IPGTT or IPITT, did not completely support the synergic effect between individual and combination treatment with IL-2C and HBO. However, combination treatment with IL-2C and HBO always represented significance.

Dyslipidemia was induced by HFD, which was also improved by the individual or combination treatment with IL-2C and HBO. Serum levels of total cholesterol were elevated by HFD, which was reduced by the individual or combination treatment with IL-2C and HBO. The size of the liver was remarkably increased to almost double and histological examination showed findings compatible with severe steatohepatitis in the HFD control groups. The combination treatment with IL-2C and HBO decreased the size of liver and improved steatohepatitis almost perfectly, in parallel with serum levels of total cholesterol. Considering that no pharmacological treatment has been approved so far for NASH, the novel findings in the present study might lead to the development of an innovative therapeutic strategy using the individual or combination treatment with IL-2C and HBO.

One of the underlying mechanisms by the individual or combination treatment with IL-2C and HBO for the altered glucose metabolism, dyslipidemia, and NASH might be related with the suppression of inflammation, while obesity is known as a systemic low-grade inflammatory state promoting the insulin resistance. F4/80⁺CD11c⁺ M1 macrophages known to dysregulate adipocyte signaling were increased in the HFD control groups locally in the adipose tissues as well as systemically in the spleen. By contrast, CD4⁺FoxP3⁺ Tregs that inhibits inflammation were decreased. Both IL-2C and HBO have been known to expand Tregs *in vivo*, in the present study, Tregs were increased by the individual or combination treatment with IL-2C and HBO locally in the adipose tissues as well as systemically in the spleen. In accordance with the increase of Tregs, M1 macrophages were decreased locally as well as systemically.

Another mechanism for the treatment effect might be related to the restoration

of hypoxia. As adipocytes become hypertrophic, it also becomes short of blood supply and hypoxia. HIF-1 α is a master mediator of hypoxic signal and is activated in obese adipose tissue. It is involved in the insulin resistance and fibrosis in the WAT [43]. Previously, it was reported that HIF-1 α in myeloid cells promoted adipose tissue remodeling toward insulin resistance [44], but selective inhibition of HIF-1 α ameliorated adipose tissue dysfunction [45]. In the liver, HIF-1 α stimulates triglyceride accumulation by stimulation of lipin 1 expression [46]. As HIF-1 α is closely linked to the glucose and lipid metabolism in both adipose tissue and liver, and therefore hyperoxia is one of the potential therapies for the treatment of hypoxia in obesity and diabetes [47]. In this study, individual treatment with HBO and combination treatment reduced HIF-1 α expression in WAT and liver in the HFD groups, suggesting the hypoxic state is alleviated. In addition, individual treatment with IL-2C also reduced HIF-1 α expression. it is not sure that how IL-2C is involved in the increase of oxygen tension in adipose tissue, but it can be speculated that weight reduction, as well as suppression of inflammation induced by treatment with IL-2C, may be related with the downregulation of HIF-1 α .

Adipose tissue undergoes dynamic remodeling such as adipocyte hypertrophy and hyperplasia, alteration of adipokine secretion, and changes in the adipose tissue-resident cells in response to the change of the nutritional status. In this study, adipocyte hypertrophy and crown-like structures were evidently shown in the HFD control groups, and it was reduced by treatment with IL-2C and HBO. It was expected that the size of adipocyte was significantly reduced by the individual or combination treatment with IL-2C and HBO, in parallel with the decrease in body weight. However, the pattern of change of the visceral adipocyte size in the

individual treatment with IL-2C was different from the expectation (Fig 3B). Nonetheless, glucose metabolism and insulin resistance were significantly improved by individual treatment with IL-2C. Furthermore, the thickness of SAT was significantly increased by HFD, and it was decreased by combination treatment with IL-2C and HBO. It was traditionally considered that VAT was the important organ for the development of insulin resistance. However, there are also studies reporting that SAT significantly influences the development of insulin resistance [48]. As SAT was increased by HFD, which was decreased by combination treatment with IL-2C and HBO, it could be considered that SAT remodeling may play an important role in the regulation of glucose and lipid metabolism.

In addition, fat browning is an important therapeutic target for non-shivering thermogenesis consuming calories. There are many studies about the relationship between BAT and glucose metabolism [49], and BAT also improves glucose homeostasis and insulin sensitivity in humans [50]. UCP-1 is an important molecule involved in the metabolic thermogenesis, and it is mainly expressed in the brown and beige adipose tissue. Interestingly, the individual or combination treatment with IL-2C and HBO in the HFD as well as LFD groups increased the UCP-1 expression at both the iBAT and iWAT. It is able to be a novel finding that the individual or combination treatment with IL-2C and HBO could be the alternative therapeutic strategy for the stimulation of fat browning.

In conclusion, the individual or combination treatment with IL-2C and HBO attenuated HFD-induced obesity and related metabolic disorders through suppression of inflammation and stimulation of fat browning. Therefore, the individual or combination treatment with IL-2C and HBO may be considered for the alternative

652 therapeutic strategy for obesity and related metabolic disorders (Fig 8).

653 **Fig. 8 Mode of action.** The individual and combination treatment of IL-2C and HBO
 654 in the prevention of HFD-induced obesity and related metabolic disorders.

Supporting information

656

657 S1 Fig. The change of body weight in LFD (A) and HFD (B) groups during 14 weeks.

658 S1 Table. Summary of the individual and synergic effects of IL-2C and HBO in the

659 HFD-induced obesity and related metabolic disorders.

References

1. Romieu I, Dossus L, Barquera S, Blottiere HM, Franks PW, Gunter M, et al. Energy balance and obesity: what are the main drivers? Cancer Causes Control. 2017; 28(3):247-58. doi: 10.1007/s10552-017-0869-z.
2. WHO, <http://www.who.int/news-room/fact-sheets/detail/obesity-and-overweight>.
3. Sahoo K, Sahoo B, Choudhury AK, Sofi NY, Kumar R, Bhadoria AS. Childhood obesity: causes and consequences. J Family Med Prim Care. 2015; 4(2):187-92. doi: 10.4103/2249-4863.154628.
4. Al-Goblan AS, Al-Alfi MA, Khan MZ. Mechanism linking diabetes mellitus and obesity. Diabetes Metab Syndr Obes. 2014; 7:587-91. Epub 2014/12/17. doi: 10.2147/DMSO.S67400.
5. Milic S, Lulic D, Stimac D. Non-alcoholic fatty liver disease and obesity: biochemical, metabolic and clinical presentations. World J Gastroenterol. 2014; 20(28):9330-7. Epub 2014/07/30. doi: 10.3748/wjg.v20.i28.9330.
6. Lovren F, Teoh H, Verma S. Obesity and atherosclerosis: mechanistic insights. Can J Cardiol. 2015; 31(2):177-83. Epub 2015/02/11. doi: 10.1016/j.cjca.2014.11.031.
7. Kachur S, Lavie CJ, de Schutter A, Milani RV, Ventura HO. Obesity and cardiovascular diseases. Minerva Med. 2017; 108(3):212-28. Epub 2017/02/06. doi: 10.23736/S0026-4806.17.05022-4.
8. Basen-Engquist K, Chang M. Obesity and cancer risk: recent review and evidence. Curr Oncol Rep. 2011; 13(1):71-6. Epub 2010/11/17. doi:

10.1007/s11912-010-0139-7.

9. Fock KM, Khoo J. Diet and exercise in management of obesity and overweight. J

Gastroenterol Hepatol. 2013; 28 Suppl 4:59-63. doi: 10.1111/jgh.12407.

10. Nguyen NT, Varela JE. Bariatric surgery for obesity and metabolic disorders:

state of the art. Nat Rev Gastroenterol Hepatol. 2017; 14(3):160-9. doi:

10.1038/nrgastro.2016.170.

11. Caterson ID. Medical management of obesity and its complications. Ann Acad

Med Singapore. 2009; 38(1):22-7. Epub 2009/02/18.

12. Golden A. Current pharmacotherapies for obesity: A practical perspective. J Am

Assoc Nurse Pract. 2017; 29(S1):S43-S52. doi: 10.1002/2327-6924.12519.

13. Boutens L, Stienstra R. Adipose tissue macrophages: going off track during

obesity. Diabetologia. 2016; 59(5):879-94. doi: 10.1007/s00125-016-3904-9.

14. Coelho M, Oliveira T, Fernandes R. Biochemistry of adipose tissue: an

endocrine organ. Arch Med Sci. 2013; 9(2):191-200. Epub 2013/05/15. doi:

10.5114/aoms.2013.33181.

15. Khan M, Joseph F. Adipose tissue and adipokines: the association with and

application of adipokines in obesity. Scientifica (Cairo). 2014; 328592. Epub

2014/10/14. doi: 10.1155/2014/328592.

16. Choe SS, Huh JY, Hwang IJ, Kim JI, Kim JB. Adipose Tissue Remodeling: Its

Role in Energy Metabolism and Metabolic Disorders. Front Endocrinol

(Lausanne). 2016; 7:30. Epub 2016/05/06. doi: 10.3389/fendo.2016.00030.

17. Bartelt A, Heeren J. Adipose tissue browning and metabolic health. Nat Rev

- Endocrinol. 2014; 10(1):24-36. Epub 2013/10/23. doi: 10.1038/nrendo.2013.204.
18. Saely CH, Geiger K, Drexel H. Brown versus white adipose tissue: a mini-review. Gerontology. 2012; 58(1):15-23. Epub 2010/12/08. doi: 10.1159/000321319.
19. Sanchez-Gurmaches J, Hung CM, Guertin DA. Emerging Complexities in Adipocyte Origins and Identity. Trends Cell Biol. 2016; 26(5):313-26. Epub 2016/02/15. doi: 10.1016/j.tcb.2016.01.004.
20. Balistreri CR, Caruso C, Candore G. The role of adipose tissue and adipokines in obesity-related inflammatory diseases. Mediators Inflamm. 2010; 802078. doi: 10.1155/2010/802078.
21. Kim SH, Plutzky J. Brown Fat and Browning for the Treatment of Obesity and Related Metabolic Disorders. Diabetes Metab J. 2016; 40(1):12-21. Epub 2016/02/26. doi: 10.4093/dmj.2016.40.1.12.
22. Oakes ND, Kjellstedt A, Thalen P, Ljung B, Turner N. Roles of Fatty Acid oversupply and impaired oxidation in lipid accumulation in tissues of obese rats. J Lipids. 2013; 420754. Epub 2013/06/14. doi: 10.1155/2013/420754.
23. Suganami T, Tanaka M, Ogawa Y. Adipose tissue inflammation and ectopic lipid accumulation. Endocr J. 2012;59(10):849-57. Epub 2012/08/11.
24. Murano I, Barbatelli G, Parisani V, Latini C, Muzzonigro G, Castellucci M, et al. Dead adipocytes, detected as crown-like structures, are prevalent in visceral fat depots of genetically obese mice. J Lipid Res. 2008; 49(7):1562-8. Epub 2008/04/09. doi: 10.1194/jlr.M800019-JLR200.
25. Asghar A, Sheikh N. Role of immune cells in obesity induced low grade

- inflammation and insulin resistance. Cell Immunol. 2017; 315:18-26. Epub 2017/03/14. doi: 10.1016/j.cellimm.2017.03.001.
26. A.M. Castro LEM-dIC, C.A. Pantoja-Meléndez. Low-grade inflammation and its relation to obesity and chronic degenerative diseases. Rev Med Hosp Gen Méx. 2017; 80(2):101-5.
27. Bell CJ, Sun Y, Nowak UM, Clark J, Howlett S, Pekalski ML, et al. Sustained *in vivo* signaling by long-lived IL-2 induces prolonged increases of regulatory T cells. J Autoimmun. 2015; 56:66-80. Epub 2014/12/03. doi: 10.1016/j.jaut.2014.10.002.
28. Anderson PM, Sorenson MA. Effects of route and formulation on clinical pharmacokinetics of interleukin-2. Clin Pharmacokinet. 1994; 27(1):19-31. Epub 1994/07/01. doi: 10.2165/00003088-199427010-00003.
29. Lee SY, Cho ML, Oh HJ, Ryu JG, Park MJ, Jhun JY, et al. Interleukin-2/anti-interleukin-2 monoclonal antibody immune complex suppresses collagen-induced arthritis in mice by fortifying interleukin-2/STAT5 signalling pathways. Immunology. 2012; 137(4):305-16. Epub 2012/11/22. doi: 10.1111/imm.12008.
30. Wang YM, Alexander SI. IL-2/anti-IL-2 complex: a novel strategy of *in vivo* regulatory T cell expansion in renal injury. J Am Soc Nephrol. 2013; 24(10):1503-4. Epub 2013/08/21. doi: 10.1681/ASN.2013070718.
31. Webster KE, Walters S, Kohler RE, Mrkvan T, Boyman O, Surh CD, et al. *In vivo* expansion of T reg cells with IL-2-mAb complexes: induction of resistance to EAE and long-term acceptance of islet allografts without immunosuppression. J Exp Med. 2009; 206(4):751-60. Epub 2009/04/01. doi: 10.1084/jem.20082824.

32. Moon BI, Kim HR, Choi EJ, Kie JH, Seoh JY. Attenuation of collagen-induced arthritis by hyperbaric oxygen therapy through altering immune balance in favor of regulatory T cells. Undersea Hyperb Med. 2017; 44(4):321-30. Epub 2017/08/08.
33. Novak S, Drenjancevic I, Vukovic R, Kellermayer Z, Cosic A, Tolusic Levak M, et al. Anti-Inflammatory Effects of Hyperbaric Oxygenation during DSS-Induced Colitis in BALB/c Mice Include Changes in Gene Expression of HIF-1alpha, Proinflammatory Cytokines, and Antioxidative Enzymes. Mediators Inflamm. 2016; 7141430. Epub 2016/09/23. doi: 10.1155/2016/7141430.
34. Tuk B, Tong M, Fijneman EM, van Neck JW. Hyperbaric oxygen therapy to treat diabetes impaired wound healing in rats. PLoS One. 2014; 9(10):e108533. Epub 2014/10/21. doi: 10.1371/journal.pone.0108533.
35. Fukaya E, Hopf HW. HBO and gas embolism. Neurol Res. 2007; 29(2):142-5. Epub 2007/04/19. doi: 10.1179/016164107X174165.
36. Gurdol F, Cimsit M, Oner-Iyidogan Y, Korpinar S, Yalcinkaya S, Kocak H. Early and late effects of hyperbaric oxygen treatment on oxidative stress parameters in diabetic patients. Physiol Res. 2008; 57(1):41-7. Epub 2007/01/17.
37. Kim HR, Kim JH, Choi EJ, Lee YK, Kie JH, Jang MH, et al. Hyperoxygenation attenuated a murine model of atopic dermatitis through raising skin level of ROS. PLoS One. 2014; 9(10):e109297. Epub 2014/10/03. doi: 10.1371/journal.pone.0109297.
38. Kim HR, Lee A, Choi EJ, Hong MP, Kie JH, Lim W, et al. Reactive oxygen species prevent imiquimod-induced psoriatic dermatitis through enhancing

- regulatory T cell function. PLoS One. 2014; 9(3):e91146. Epub 2014/03/13. doi:
10.1371/journal.pone.0091146.
39. Tsuneyama K, Chen YC, Fujimoto M, Sasaki Y, Suzuki W, Shimada T, et al.
Advantages and disadvantages of hyperbaric oxygen treatment in mice with
obesity hyperlipidemia and steatohepatitis. ScientificWorldJournal. 2011;
11:2124-35. doi: 10.1100/2011/380236.
40. Wilkinson D, Chapman IM, Heilbronn LK. Hyperbaric oxygen therapy improves
peripheral insulin sensitivity in humans. Diabet Med. 2012; 29(8):986-9. doi:
10.1111/j.1464-5491.2012.03587.x.
41. Wilkinson D, Nolting M, Mahadi MK, Chapman I, Heilbronn L. Hyperbaric oxygen
therapy increases insulin sensitivity in overweight men with and without type 2
diabetes. Diving Hyperb Med. 2015; 45(1):30-6.
42. Takahashi Y, Fukusato T. Histopathology of nonalcoholic fatty liver
disease/nonalcoholic steatohepatitis. World J Gastroenterol. 2014;
20(42):15539-48. Epub 2014/11/18. doi: 10.3748/wjg.v20.i42.15539.
43. Halberg N, et al.,. Hypoxia-inducible factor 1 alpha induces fibrosis and insulin
resistance in white adipose tissue. Mol cell biol. 2009; 29(16):4467-83.
44. Takikawa A, Mahmood A, Nawaz A, Kado T, Okabe K, Yamamoto S, et al. HIF-
1alpha in Myeloid Cells Promotes Adipose Tissue Remodeling Toward Insulin
Resistance. Diabetes. 2016; 65(12):3649-59. Epub 2016/09/15. doi:
10.2337/db16-0012.
45. Sun K, Halberg N, Khan M, Magalang UJ, Scherer PE. Selective inhibition of
hypoxia-inducible factor 1alpha ameliorates adipose tissue dysfunction. Mol Cell

Biol. 2013; 33(5):904-17. Epub 2012/12/20. doi: 10.1128/MCB.00951-12.

46. Mylonis I, Sembongi H, Befani C, Liakos P, Siniossoglou S, Simos G. Hypoxia causes triglyceride accumulation by HIF-1-mediated stimulation of lipin 1 expression. J Cell Sci. 2012; 125(Pt 14):3485-93. Epub 2012/04/03. doi: 10.1242/jcs.106682.

47. Norouzirad R, Gonzalez-Muniesa P, Ghasemi A. Hypoxia in Obesity and Diabetes: Potential Therapeutic Effects of Hyperoxia and Nitrate. Oxid Med Cell Longev. 2017; 5350267. Epub 2017/06/14. doi: 10.1155/2017/5350267.

48. Patel P AN. Role of subcutaneous adipose tissue in the pathogenesis of insulin resistance. J Obes 2013; 489187. doi: 10.1155/2013/489187.

49. Stanford KI MR, Townsend KL, An D, Nygaard EB, Hitchcox KM, Markan KR, Nakano K, Hirshman MF, Tseng YH, Goodyear LJ. Brown adipose tissue regulates glucose homeostasis and insulin sensitivity. J Clin Invest. 2013; 123(1):215-23. doi: 10.1172/JCI62308.

50. Chondronikola M, Volpi E, Borsheim E, Porter C, Annamalai P, Enerback S, et al. Brown adipose tissue improves whole-body glucose homeostasis and insulin sensitivity in humans. Diabetes. 2014; 63(12):4089-99. Epub 2014/07/25. doi: 10.2337/db14-0746.

D

LFD

HFD

NT

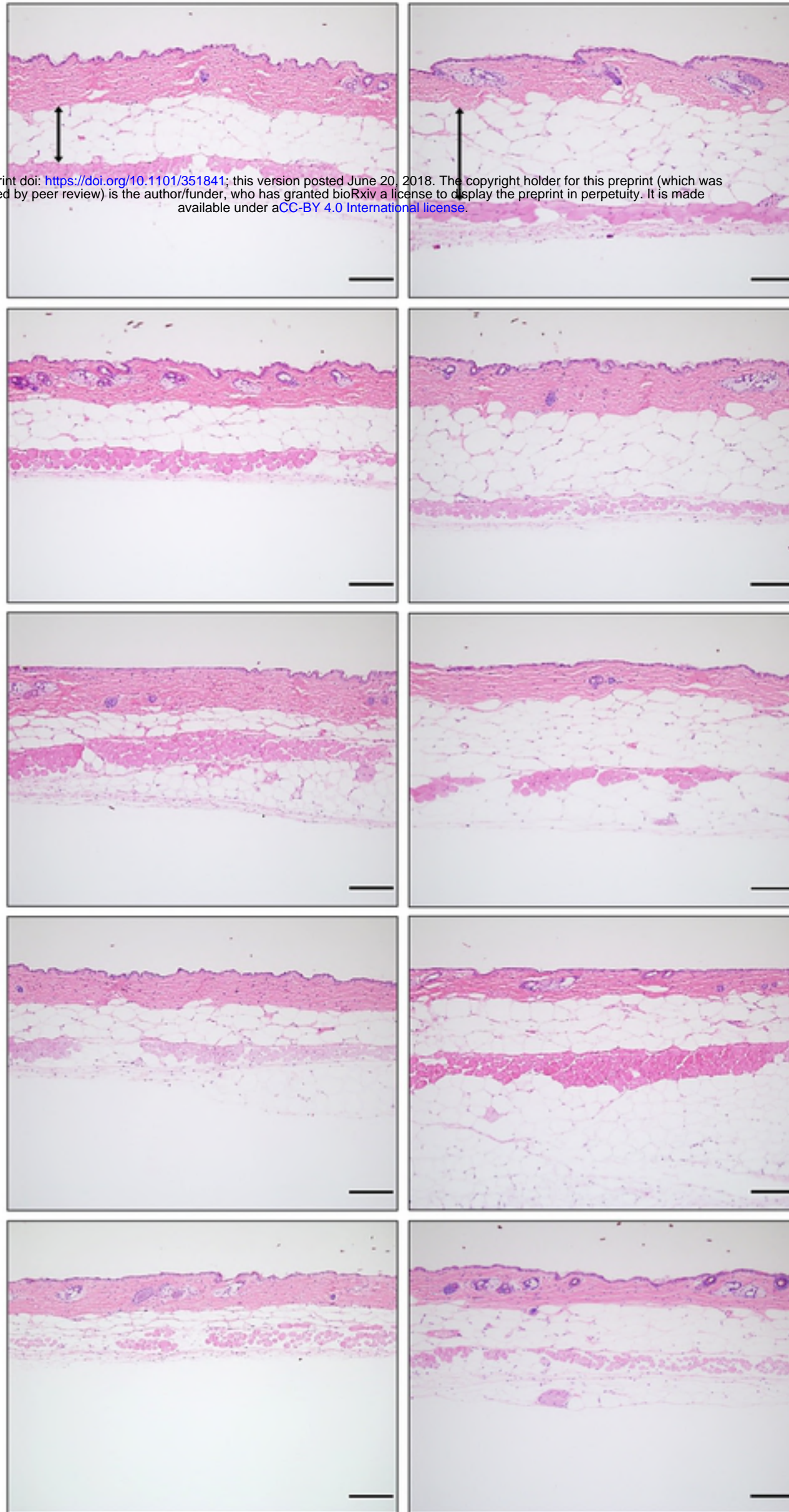
bioRxiv preprint doi: <https://doi.org/10.1101/351841>; this version posted June 20, 2018. The copyright holder for this preprint (which was not certified by peer review) is the author/funder, who has granted bioRxiv a license to display the preprint in perpetuity. It is made available under aCC-BY 4.0 International license.

PBS

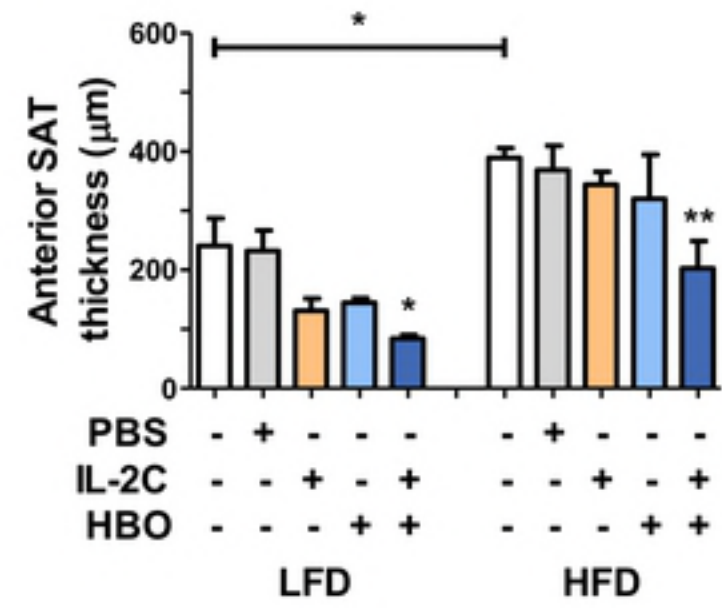
IL-2C

HBO

**IL-2C
+
HBO**



E



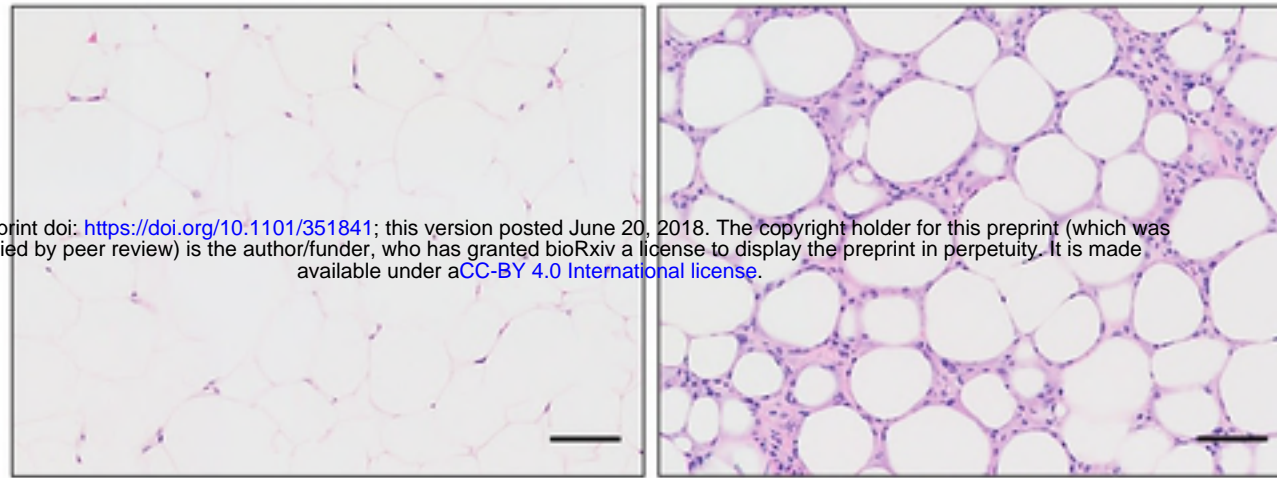
A

LFD

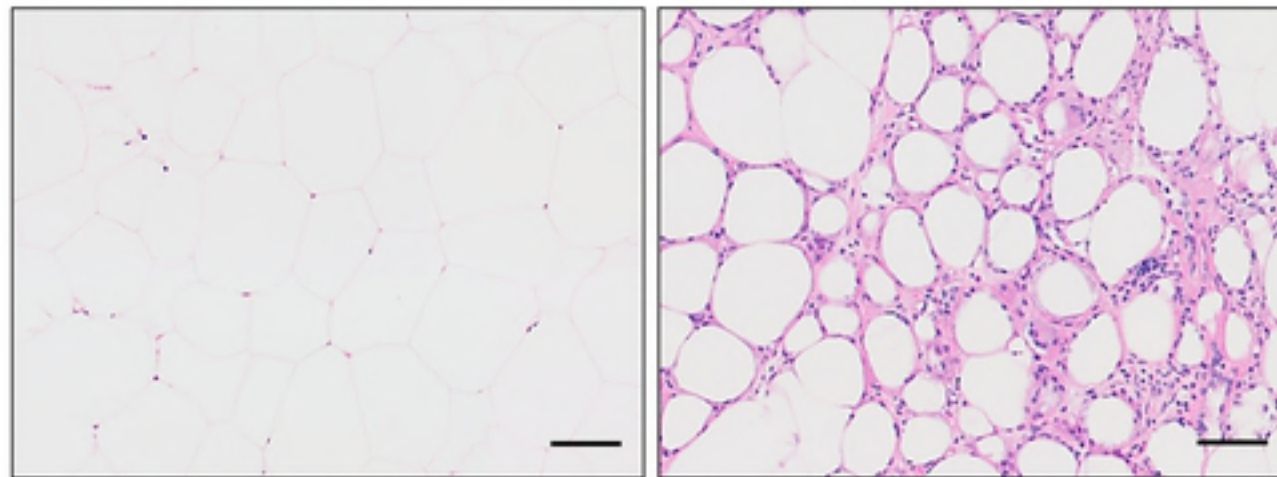
HFD

bioRxiv preprint doi: <https://doi.org/10.1101/351841>; this version posted June 20, 2018. The copyright holder for this preprint (which was not certified by peer review) is the author/funder, who has granted bioRxiv a license to display the preprint in perpetuity. It is made available under aCC-BY 4.0 International license.

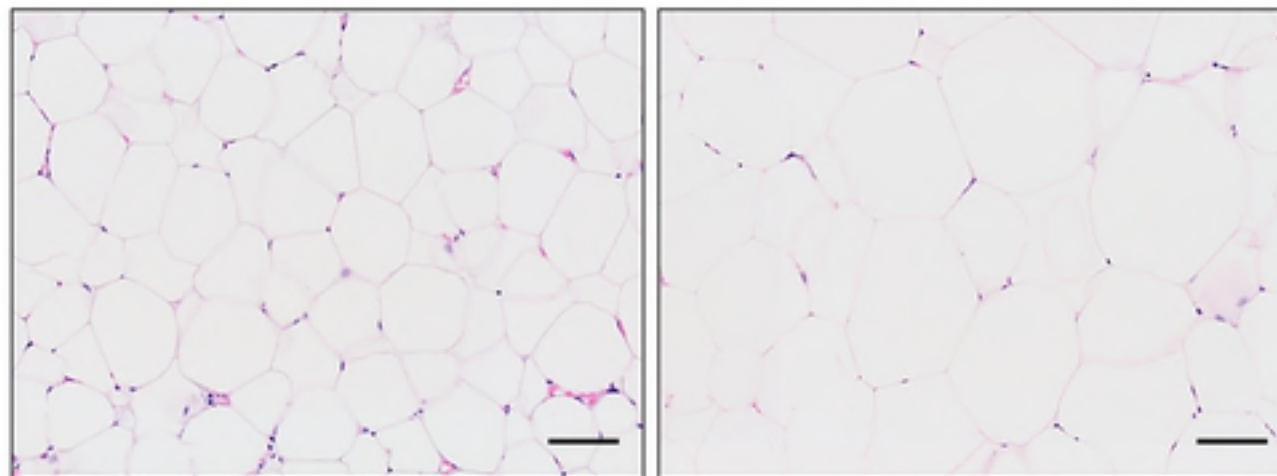
NT



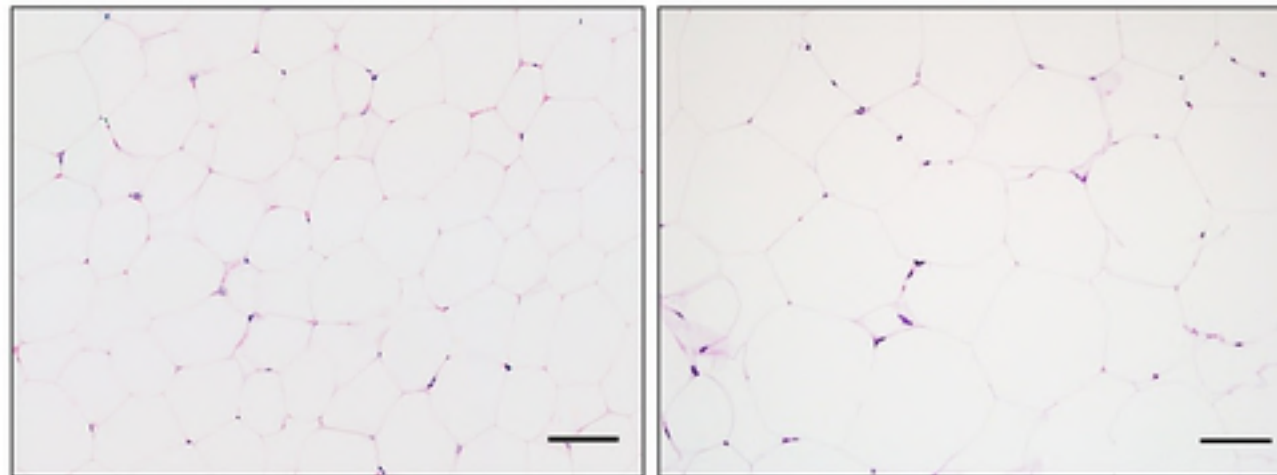
PBS



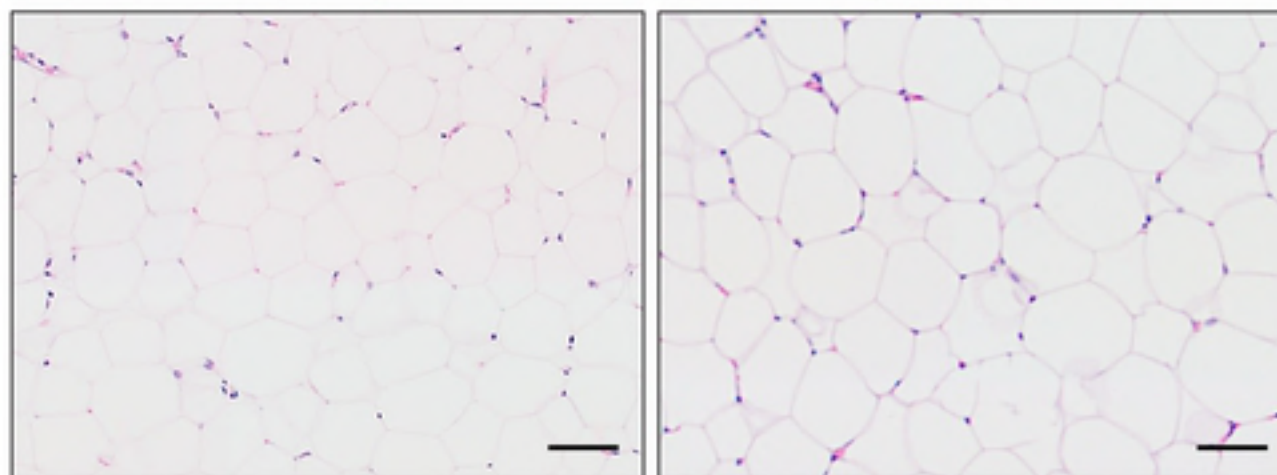
IL-2C



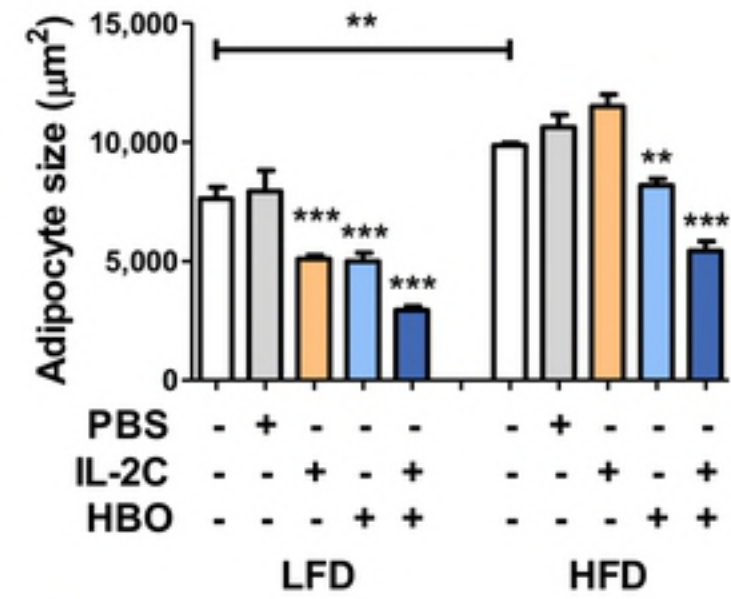
HBO



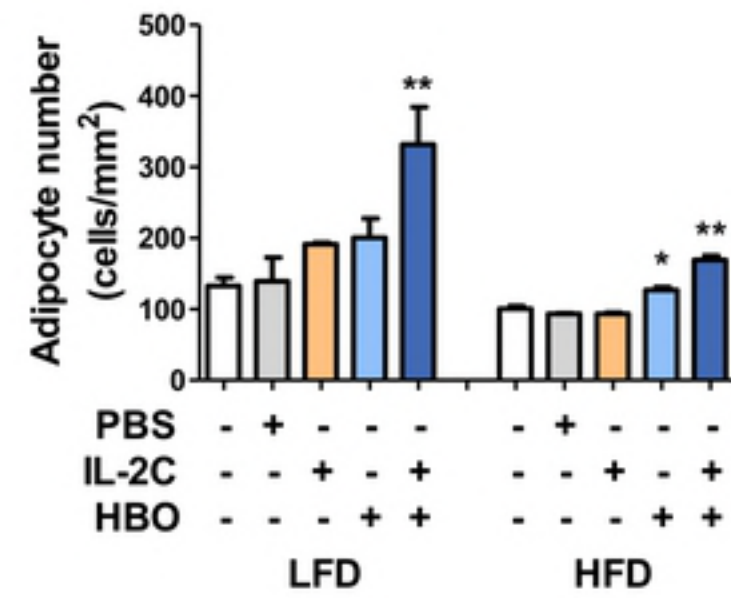
**IL-2C
+
HBO**

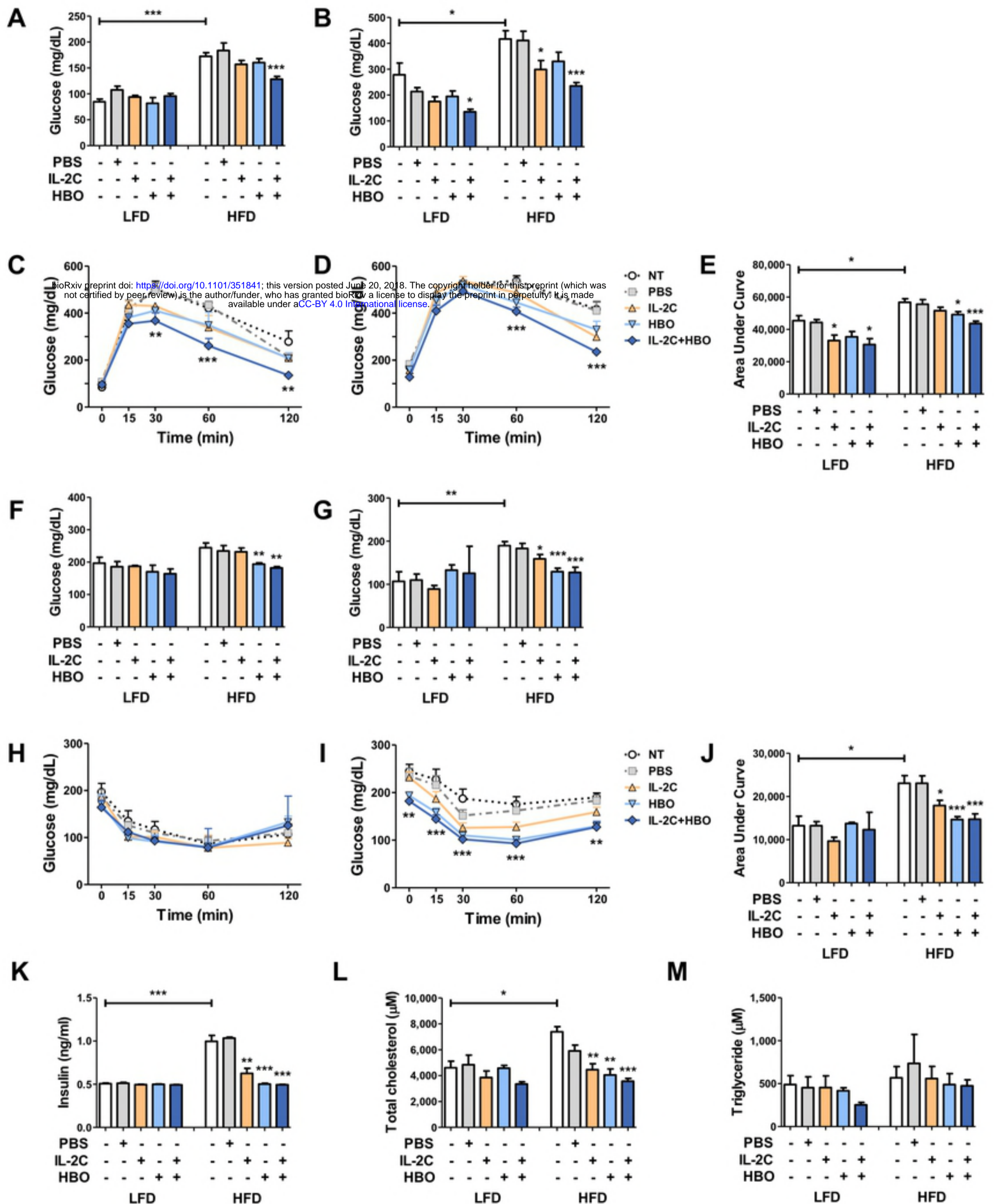


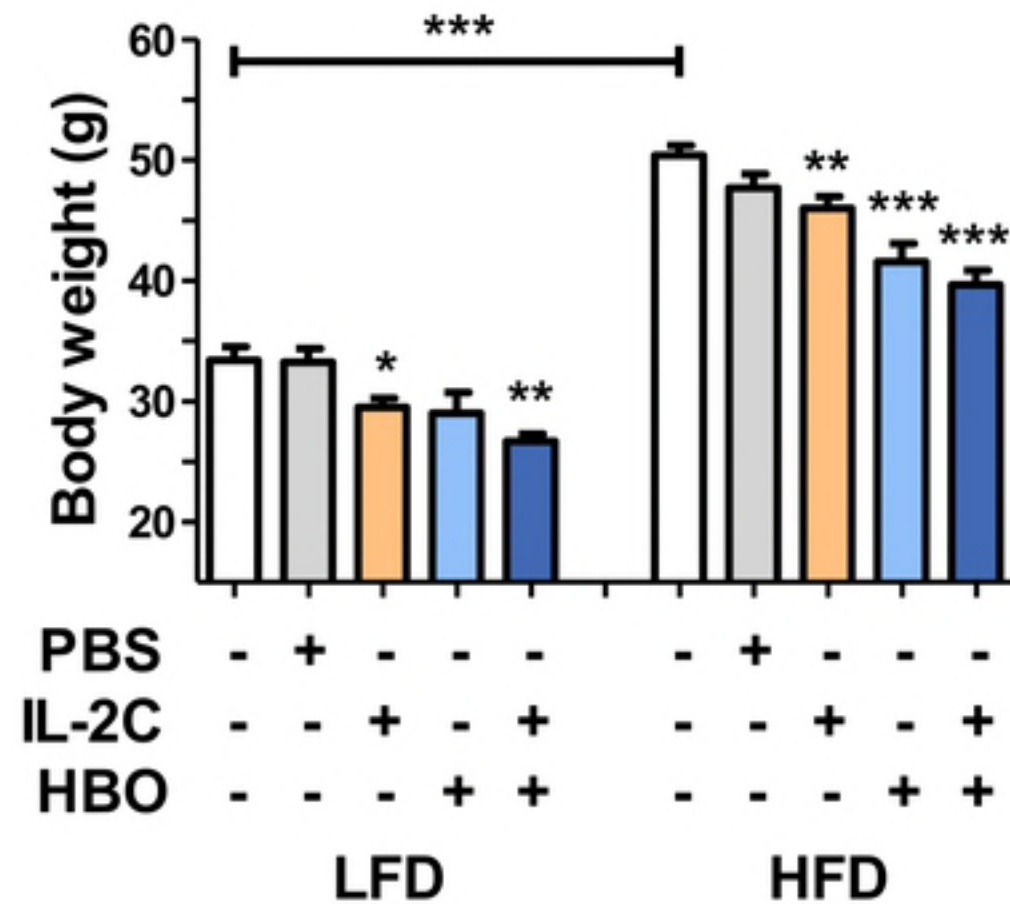
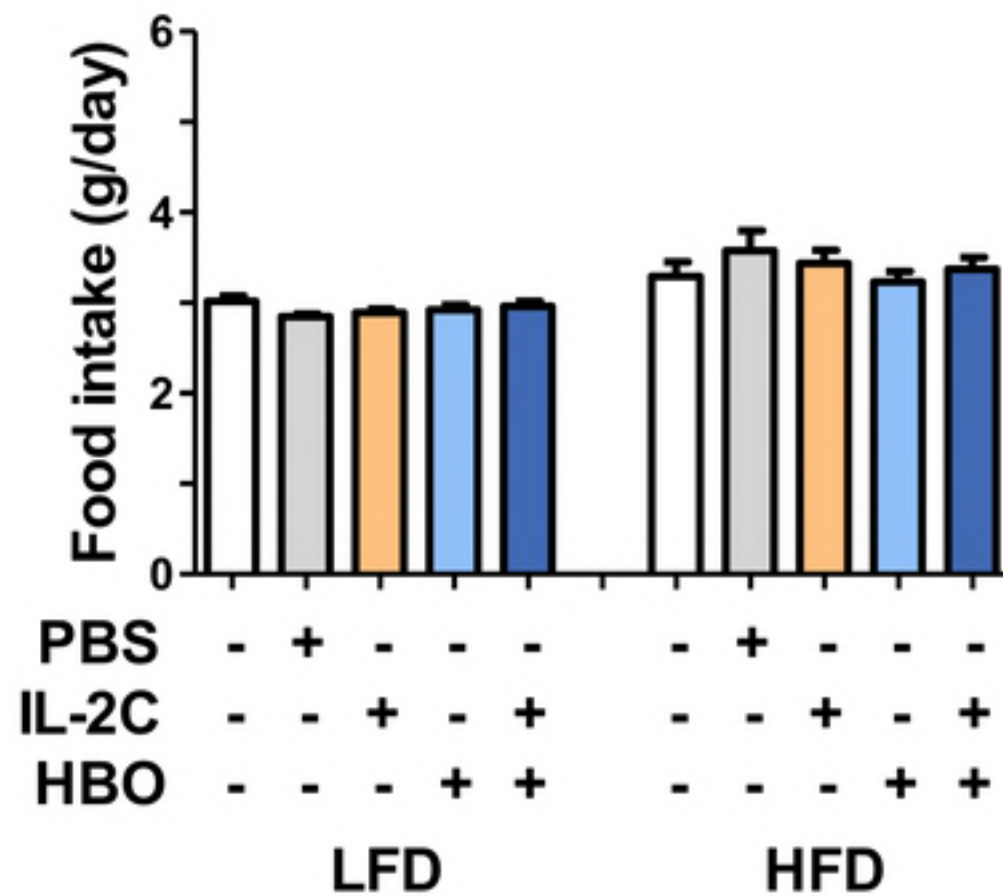
B

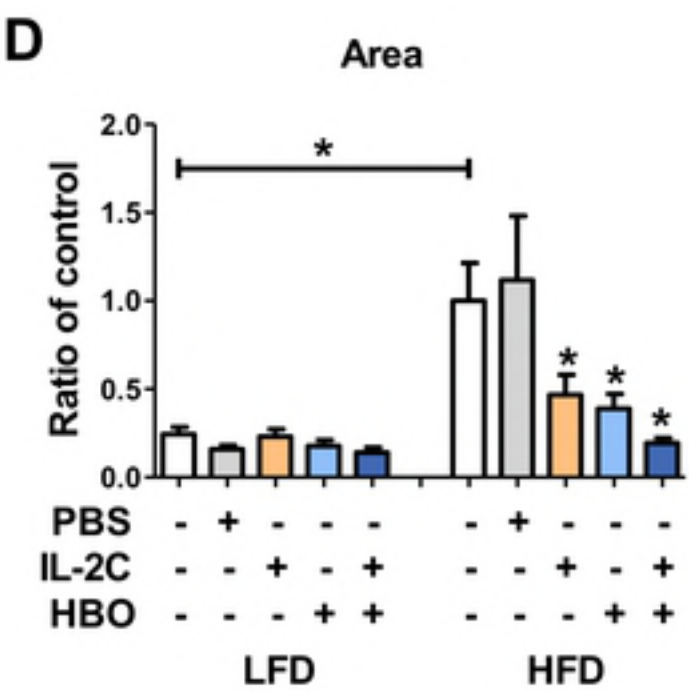
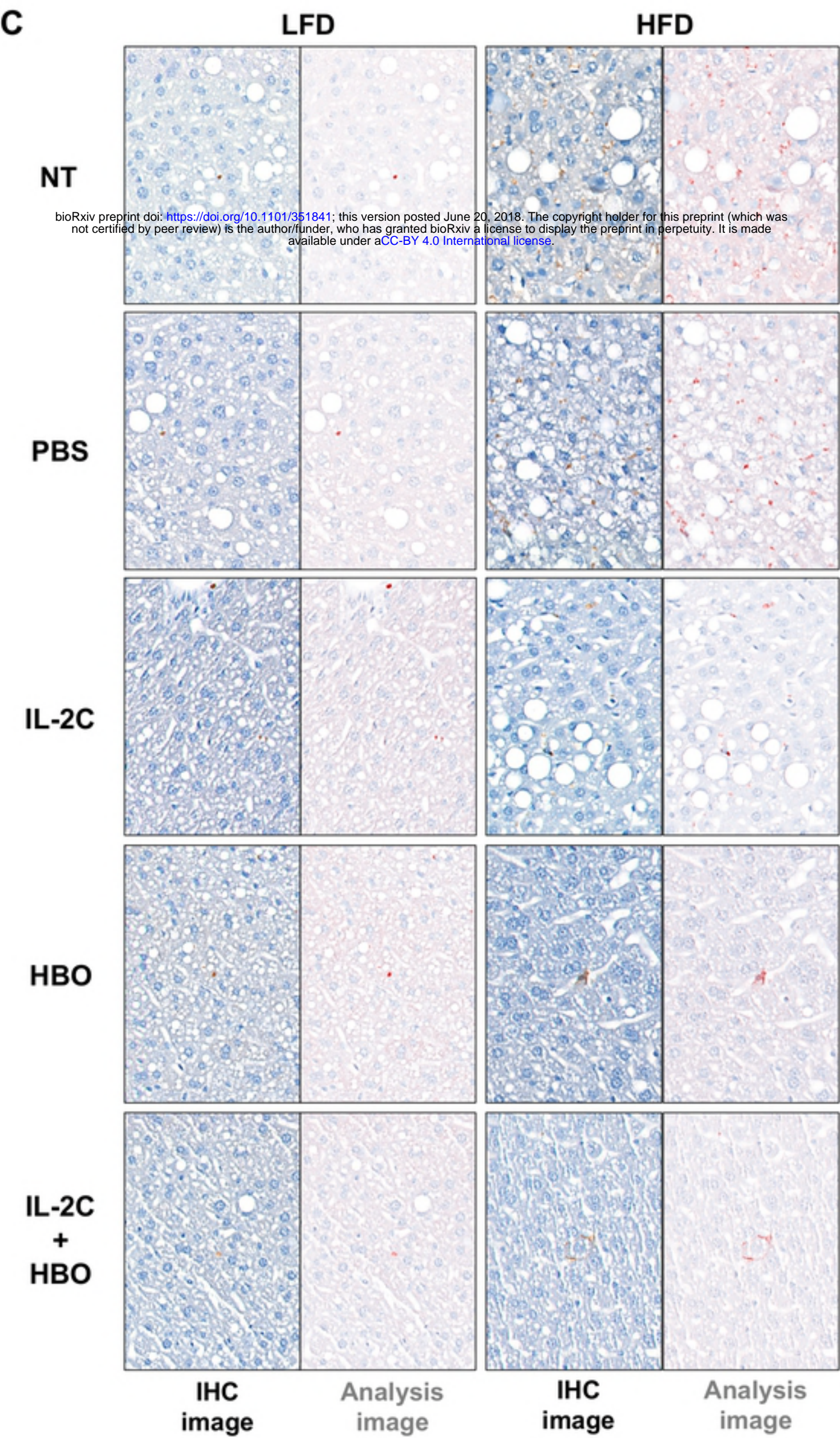


C





A**B**



A

LFD

HFD

B

Area

NT

PBS

IL-2C

HBO

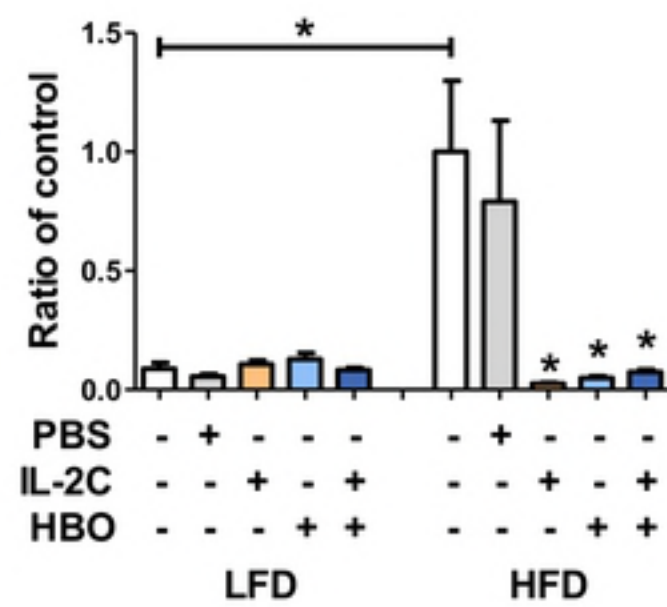
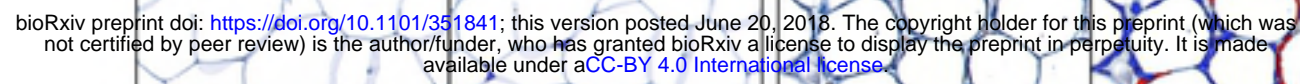
**IL-2C
+
HBO**

IHC
image

Analysis
image

IHC
image

Analysis
image



A

LFD

HFD

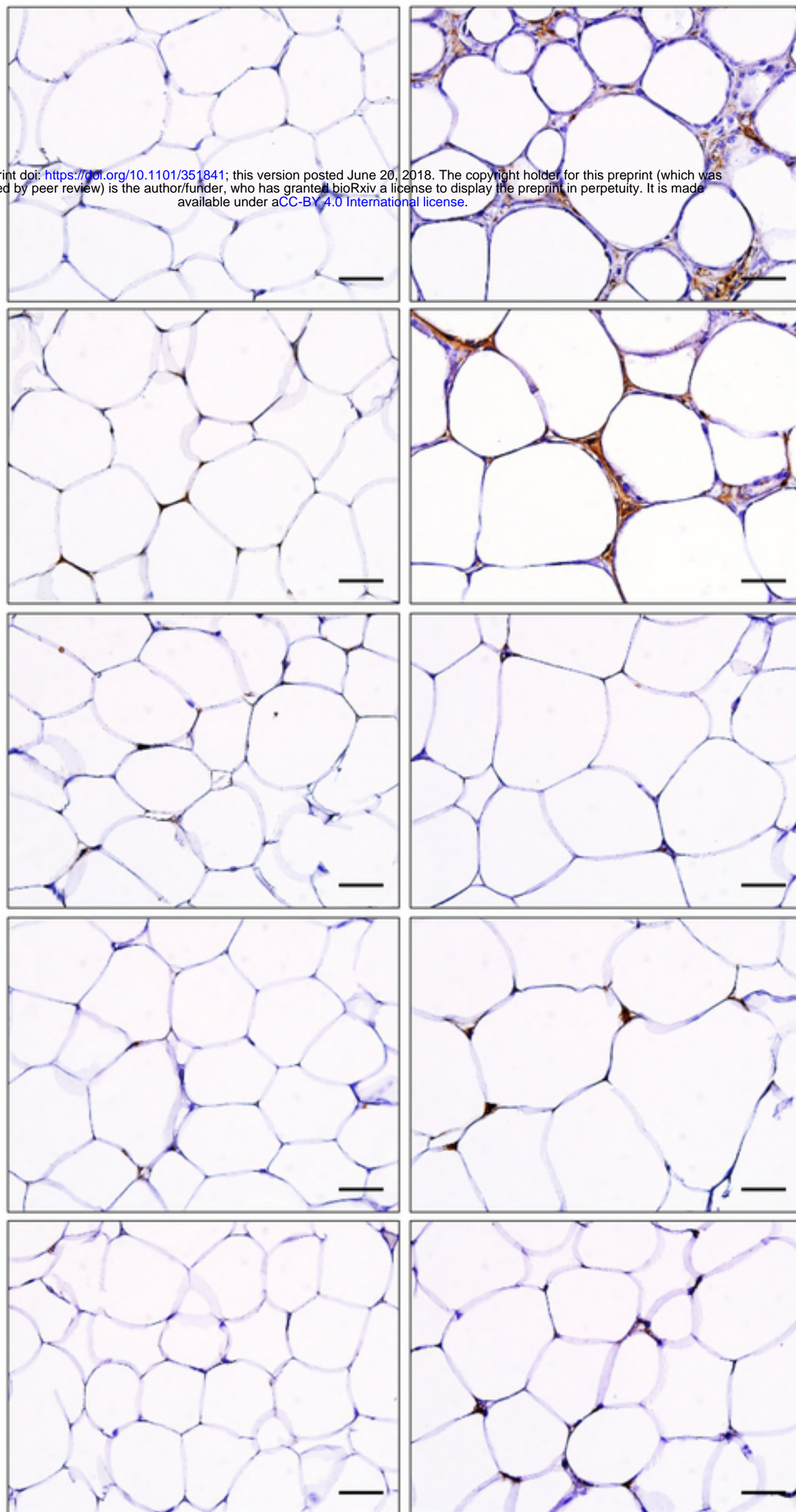
NT

bioRxiv preprint doi: <https://doi.org/10.1101/351841>; this version posted June 20, 2018. The copyright holder for this preprint (which was not certified by peer review) is the author/funder, who has granted bioRxiv a license to display the preprint in perpetuity. It is made available under aCC-BY 4.0 International license.

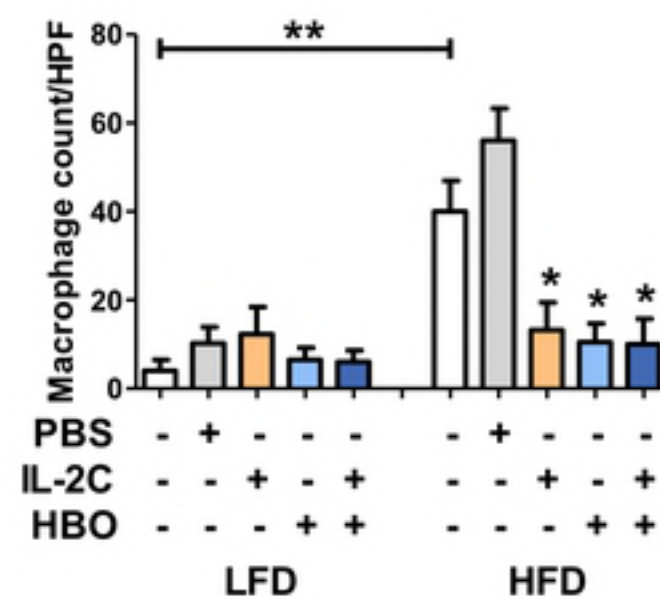
PBS

IL-2C

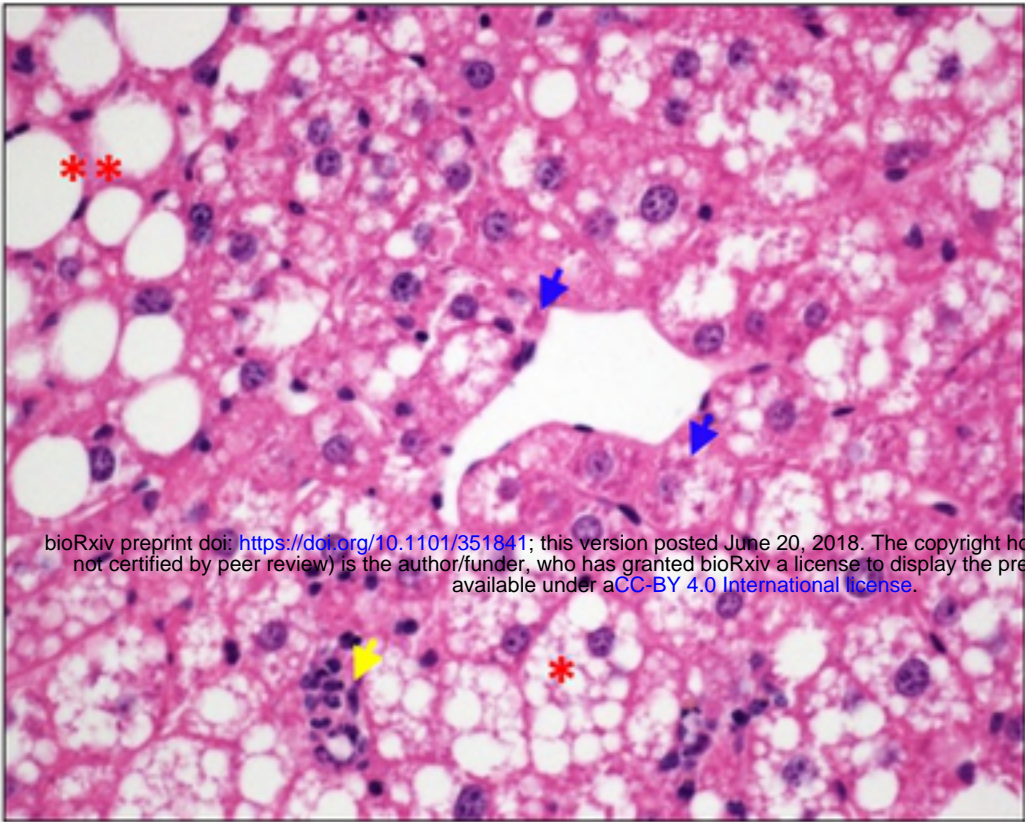
HBO

 IL-2C
+
HBO


B



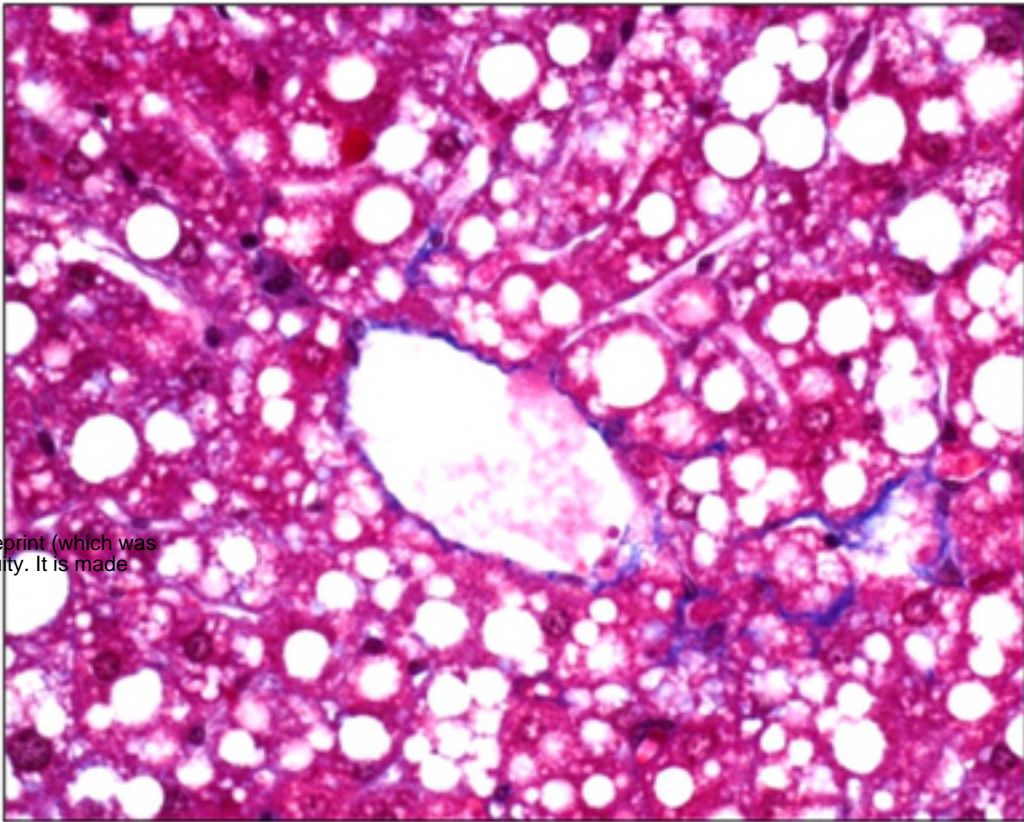
D



bioRxiv preprint doi: <https://doi.org/10.1101/351841>; this version posted June 20, 2018. The copyright holder for this preprint (which was not certified by peer review) is the author/funder, who has granted bioRxiv a license to display the preprint in perpetuity. It is made available under aCC-BY 4.0 International license.

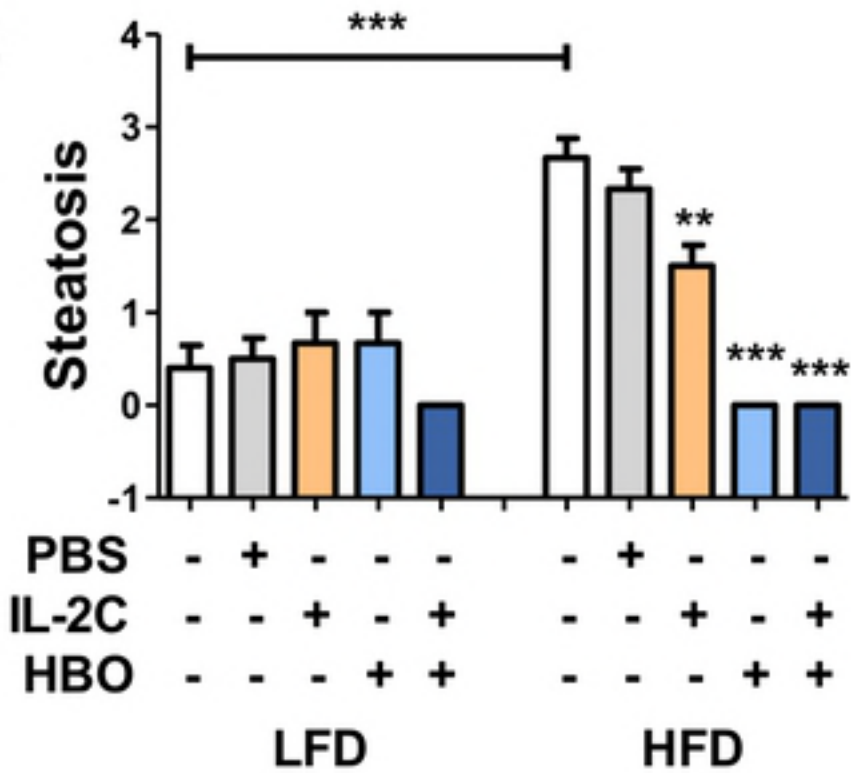
H&E, X400

E

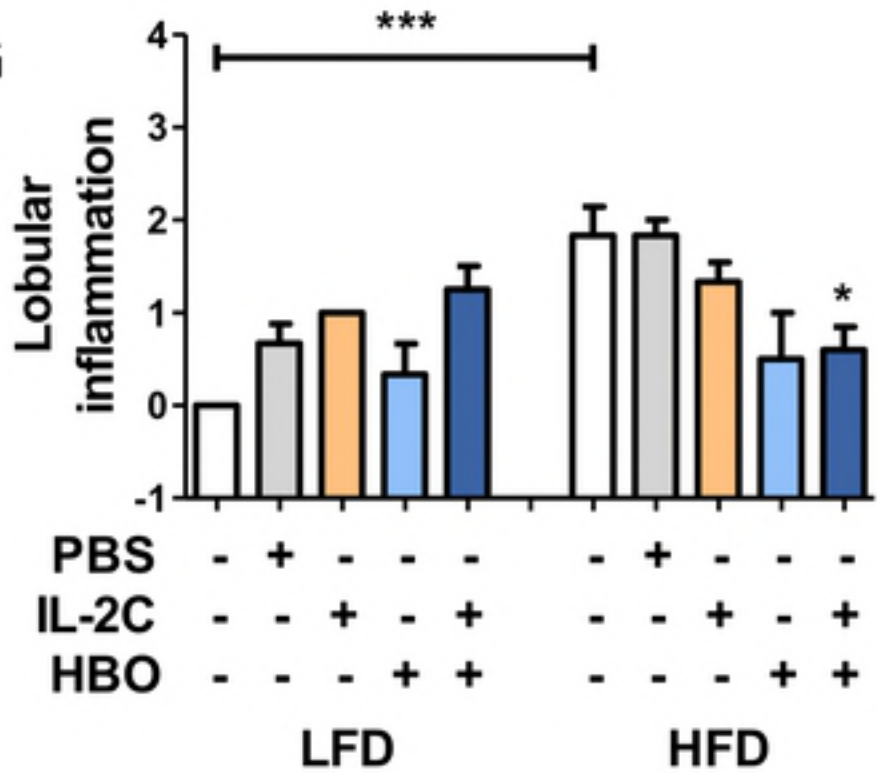


TRC, X400

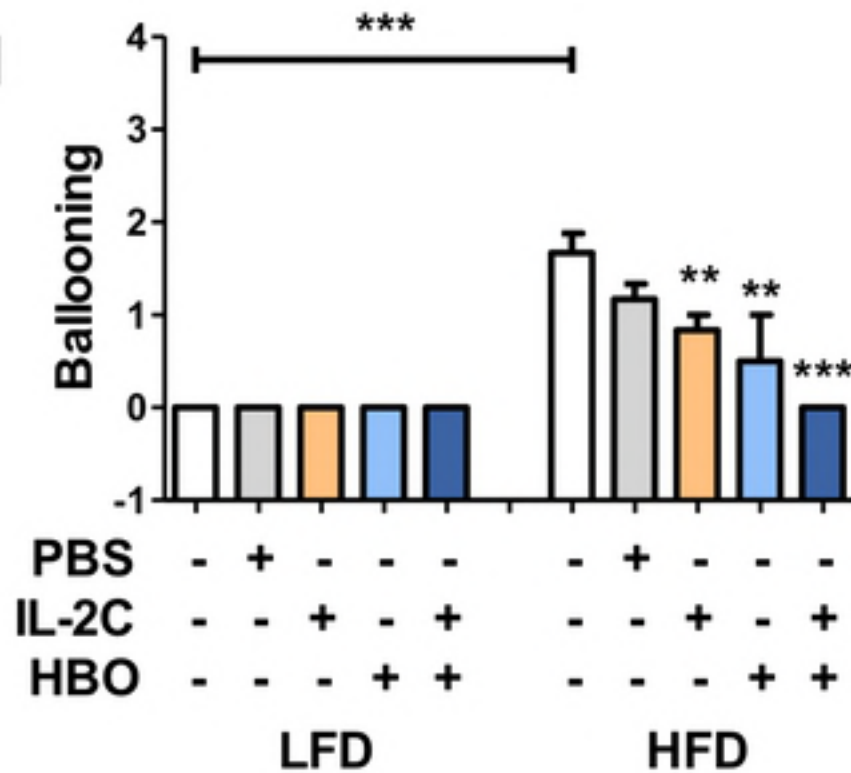
F



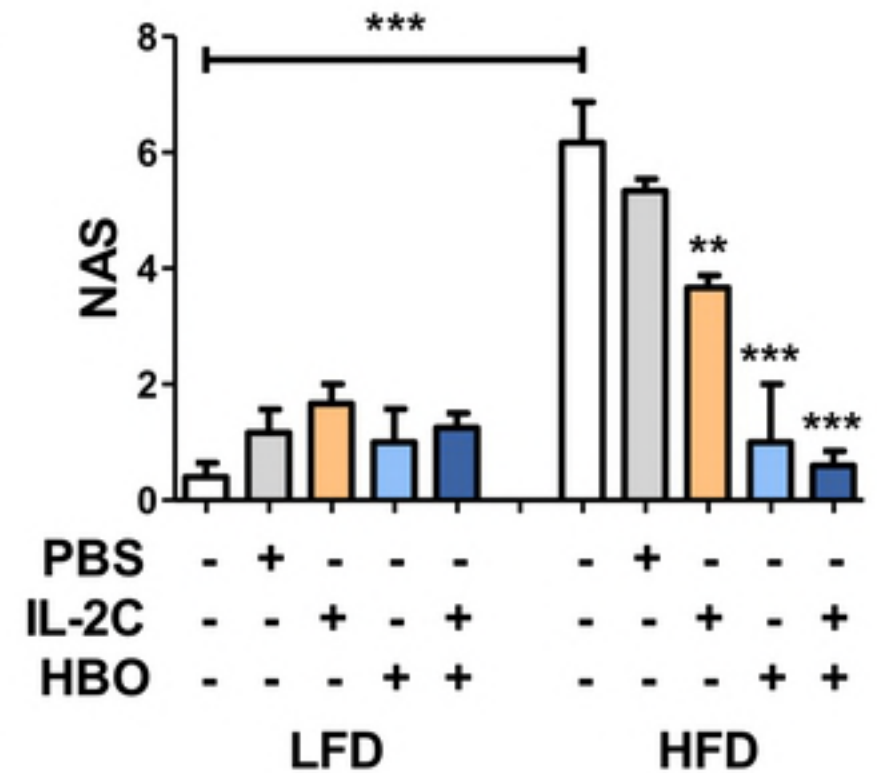
G

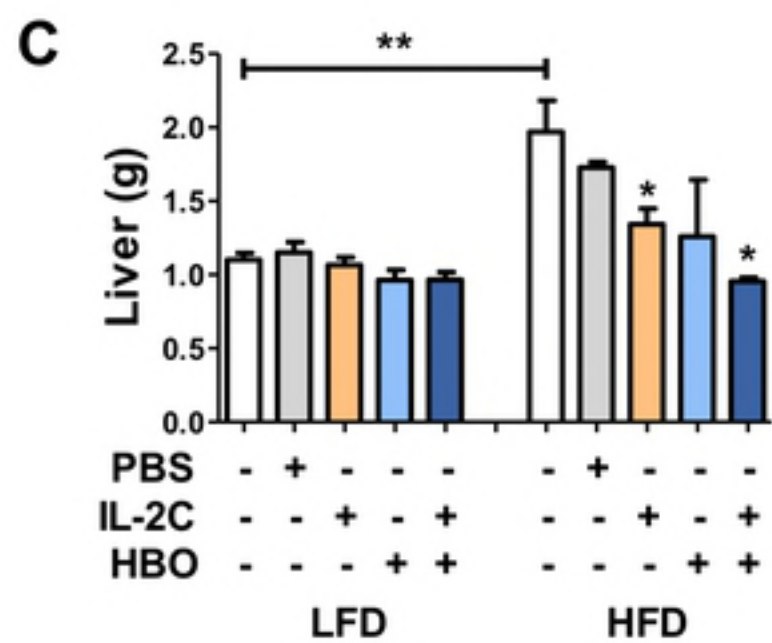
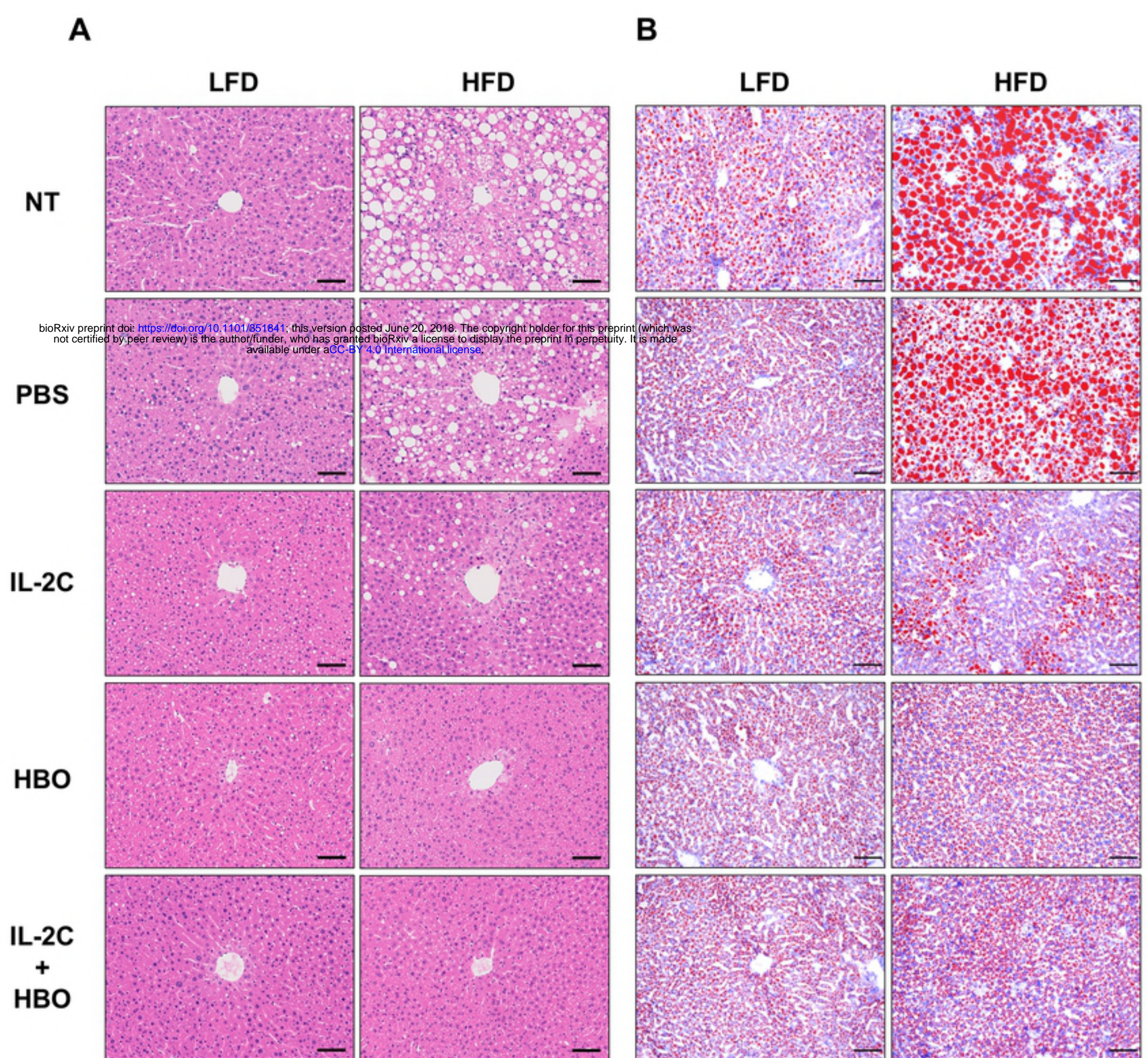


H



I





Obesity

Obesity related metabolic disorders

Obesity induced Immuno-pathogenesis cycle

